

Quark model study of the $\pi N \rightarrow \pi N$ reactions up to the $N(1440)$ resonance region

Kai-Lei Wang, Li-Ye Xiao, Xian-Hui Zhong *

1) Department of Physics, Hunan Normal University, and Key Laboratory of Low-Dimensional Quantum Structures and Quantum Control of Ministry of Education, Changsha 410081, China and

2) Synergetic Innovation Center for Quantum Effects and Applications (SICQEA), Hunan Normal University, Changsha 410081, China

A combined analysis of the reactions $\pi^+ p \rightarrow \pi^+ p$, $\pi^- p \rightarrow \pi^- p$ and $\pi^- p \rightarrow \pi^0 n$ is carried out with a chiral quark model. The observations are reasonably described from the $\Delta(1232)$ resonance region up to the $N(1440)$ resonance region. Besides the $\Delta(1232)P_{33}$, a confirmed role of $N(1440)P_{11}$ is found in the polarizations of the $\pi^- p \rightarrow \pi^- p$ and $\pi^- p \rightarrow \pi^0 n$ reactions. It is found that the $N(1440)N\pi$ and $\Delta(1232)N\pi$ couplings are about 1.7 and 4.8 times larger than the expectations from the simple quark model, respectively, which may suggest the unusual property of $N(1440)P_{11}$ and deficiency of the simple quark model in the description of $N(1440)P_{11}$ and $\Delta(1232)P_{33}$. The t - and u -channel backgrounds have notable contributions to the $\pi^+ p \rightarrow \pi^+ p$ reaction, while in the $\pi^- p \rightarrow \pi^- p, \pi^0 n$ reactions, the s -channel nucleon and t - and u -channel backgrounds play crucial roles.

PACS numbers: 12.39.Jh, 13.75.Gx, 14.20.Gk

I. INTRODUCTION

A better understanding of the baryon spectrum and internal structure of excited baryons is a fundamental challenge and goal in hadronic physics [1–3]. Pion-nucleon (πN) scattering provides us an important place to study the Δ and nucleon spectroscopies. Most of our current knowledge about the Δ and nucleon resonances listed in the Review of Particle Physics by the Partial Data Group (PDG) [4] was extracted from the πN scattering. In the past decades, although many efforts have been made by several partial wave analysis groups [5–27], the properties of some Δ and nucleon resonances are not well understood. Still, strong model dependencies exist in the extracted resonance properties from different groups. For example, the study of πN scattering in the literature [11, 12] indicates that the Roper $N(1440)P_{11}$ is dynamically generated from the coupled channel interaction without any excited three-quark core, while in the literature [26–28] the Roper $N(1440)P_{11}$ is suggested to be a three-quark state dressed by a meson cloud. Furthermore, in some literature the $N(1535)S_{11}$ resonance is suggested to be a dynamically generated resonance by analyzing the πN reactions [29–33]. Recently, according to our chiral quark model study of the $\pi^- p \rightarrow \eta n, K^+ \Lambda$ [34, 35], and $\gamma N \rightarrow \eta N, \pi^0 N$ reactions [36, 37], the $N(1535)S_{11}$ resonance can be explained as a mixing three-quark state between representations of [70, ²8] and [70, ⁴8]. To deepen our understanding of the resonance properties from the πN reactions, more partial wave analyses are needed.

In present work, we further extend the chiral quark model to the study of the π^\pm elastic reactions $\pi^+ p \rightarrow \pi^+ p$, $\pi^- p \rightarrow \pi^- p$ and the charge-exchange reaction $\pi^- p \rightarrow \pi^0 n$ up to the $N(1440)$ resonance region. The $\pi N \rightarrow \pi N$ reactions provide us a good place to study the $\Delta(1232)P_{33}$ and $N(1440)P_{11}$, because the other higher resonances, such as $N(1535)S_{11}$ and $\Delta(1620)S_{31}$ are far from the $\Delta(1232)$ and $N(1440)$ region, their interferences in this low energy region should be strongly

suppressed by the phase space. On the other hand, in the energy regions what we will consider, there are abundant data, which have been collected by the GWU group [38]. By a combined analysis of these reactions, we hope (i) to further test the validity of the chiral quark model and obtain a better understanding of the reaction mechanism for the πN scattering; (ii) to confirm the properties of $\Delta(1232)P_{33}$ extracted from the π^0 -meson photoproduction processes in our previous work [36]; (iii) to extract some reliable information of $N(1440)P_{11}$. In our previous quark model analyses of the $\pi^- p \rightarrow \eta n, K^+ \Lambda$ [34, 35] and $\gamma N \rightarrow \eta N, \pi^0 N$ [36, 37] reactions, no obvious evidence of $N(1440)P_{11}$ is found.

In the chiral quark model, an effective chiral Lagrangian is introduced to account for the quark-pseudoscalar-meson coupling. Since the quark-meson coupling is invariant under the chiral transformation, some of the low-energy properties of QCD are retained. There are several outstanding features for this model [35, 39, 40]. One is that in this framework only one overall parameter is needed for the nucleon resonances to be coupled to the pseudoscalar mesons in the $SU(6) \otimes O(3)$ symmetry limit. This is distinguished from hadronic models where each resonance requires one additional coupling constant as free parameter. Furthermore, the s - and u -channel transition amplitudes at the tree level can be explicitly calculated, and the quark model wavefunctions for the baryon resonances, after convolution integrals, provide a form factor for the interaction vertices. Consequently, all the baryon resonances can be consistently included. The chiral quark model has been well developed and successfully applied to pseudoscalar-meson photoproduction reactions [36, 37, 39–50]. Recently, this model has been extended to $\pi^- p$ [34, 35] and $K^- p$ [51–53] reactions as well, which provides some novel insights into the observables measured in these reactions.

This work is organized as follows. The model is reviewed in Sec.II. Then, in Sec.III, our numerical results and analysis are presented and discussed. Finally, a summary is given in Sec.IV.

*E-mail: zhongxh@hunnu.edu.cn

II. FRAMEWORK

In this section, we give a brief review of the chiral quark model. In this model, the meson-quark interactions are adopted by the effective chiral Lagrangian [40]

$$H_m = \frac{1}{f_m} \bar{\psi}_j \gamma_\mu^j \gamma_5^j \psi_j \vec{\tau} \cdot \partial^\mu \vec{\phi}_m, \quad (1)$$

where ψ_j represents the j -th quark field in a hadron, f_m is the meson's decay constant, and ϕ_m is the field of the pseudoscalar-meson octet. Then the s - and u -channel transition amplitudes \mathcal{M}_s and \mathcal{M}_u can be worked out with the relations [35]:

$$\mathcal{M}_s = \sum_j \langle N_f | H_m^f | N_j \rangle \langle N_j | \frac{1}{E_i + \omega_i - E_j} H_m^i | N_i \rangle, \quad (2)$$

$$\mathcal{M}_u = \sum_j \langle N_f | H_m^i \frac{1}{E_i - \omega_i - E_j} | N_j \rangle \langle N_j | H_m^f | N_i \rangle. \quad (3)$$

In the above equations, the ω_i and ω_f are the energies of the incoming and outgoing mesons, respectively. $|N_i\rangle$, $|N_j\rangle$ and $|N_f\rangle$ stand for the initial, intermediate, and final states, respectively, and their corresponding energies E_i , E_j , and E_f are the eigenvalues of the nonrelativistic Hamiltonian of the constituent quark model \hat{H} [54–56]. In our previous work [35, 52], the amplitudes \mathcal{M}_s and \mathcal{M}_u have been worked out in the harmonic oscillator basis.

The t -channel backgrounds might play an important role in the reactions, thus, the t -channel contributions of vector exchange and the scalar exchange are considered in this work. The vector meson-quark and scalar meson-quark interactions are adopted by [34]

$$H_V = \bar{\psi}_j \left(a \gamma^\nu + \frac{b \sigma^{\nu\lambda} \partial_\lambda}{2m_q} \right) V_\nu \psi_j, \quad (4)$$

$$H_S = g_{Sqq} \bar{\psi}_j \psi_j S. \quad (5)$$

Meanwhile, the VPP and SPP couplings are adopted as

$$H_{VPP} = -iG_V \text{Tr}([\phi_m, \partial_\mu \phi_m] V^\mu), \quad (6)$$

$$H_{SPP} = \frac{g_{SPP}}{2m_\pi} \partial_\mu \phi_m \partial^\mu \phi_m \quad (7)$$

where V , P and S stand for the vector-, pseudoscalar-, scalar-meson fields, respectively. The coupling constants a , b , g_{Sqq} , G_V , and g_{SPP} are to be determined by experimental data. In this work, both the scalar σ - and vector ρ -meson exchanges are considered for the $\pi^+ p \rightarrow \pi^+ p$ and $\pi^- p \rightarrow \pi^- p$ processes, while the vector ρ -meson exchange is only considered for the $\pi^- p \rightarrow \pi^0 p$ process. The details of the t -channel transition amplitude can be found in our previous work [53].

Furthermore, the backgrounds from the Coulomb interactions and the contact term maybe play some roles in the reactions at low energies. To include the contributions from the contact term (meson-meson-quark-quark interaction), we adopt an effective chiral Lagrangian [57]:

$$H_{\text{contact}} = \frac{i}{4f_m^2} \bar{\psi}_j \gamma^\mu [[\phi_m, (\partial_\mu \phi_m)], \psi_j], \quad (8)$$

To include the contributions of Coulomb interactions, we follow the method developed in Refs. [58–61]. The details of the amplitudes for the Coulomb term can be found in Ref. [61].

In this work, we focus on the contributions of the s -channel resonances, which are degenerate within the same principle number n . To obtain the contributions of individual resonances, we need to separate out the single-resonance-excitation amplitudes within each principle number n in the s channel. Taking into account the width effects of the resonances, the resonance transition amplitudes of s channel can be generally expressed as [35, 53]

$$\mathcal{M}_R^s = \frac{2M_R}{s - M_R^2 + iM_R\Gamma_R} O_R e^{-(\mathbf{k}^2 + \mathbf{q}^2)/6\alpha^2}, \quad (9)$$

where $\sqrt{s} = E_i + \omega_i$ is the total energy of the system, \mathbf{k} and \mathbf{q} stand for the momenta of incoming and outgoing mesons, α is the harmonic oscillator strength, and O_R is the separated operators for individual resonances. M_R is the mass of the s -channel resonance with a width Γ_R . The transition amplitude can be written in a standard form [62]:

$$O_R = f(\theta) + ig(\theta)\boldsymbol{\sigma} \cdot \mathbf{n}, \quad (10)$$

where $\boldsymbol{\sigma}$ is the spin operator of the nucleon, $\mathbf{n} \equiv \mathbf{q} \times \mathbf{k} / |\mathbf{k} \times \mathbf{q}|$. $f(\theta)$ and $g(\theta)$ stand for the non-spin-flip and spin-flip amplitudes, respectively, which can be expanded in terms of the familiar partial wave amplitudes $T_{l\pm}$ for the states with $J = l \pm 1/2$:

$$f(\theta) = \sum_{l=0}^{\infty} [(l+1)T_{l+} + lT_{l-}] P_l(\cos \theta), \quad (11)$$

$$g(\theta) = \sum_{l=0}^{\infty} [T_{l-} - T_{l+}] \sin \theta P_l'(\cos \theta). \quad (12)$$

Both the isospin- $\frac{1}{2}$ and isospin- $\frac{3}{2}$ resonances contribute to the $\pi^- p \rightarrow \pi^- p, \pi^0 n$ reactions. Thus, we need separate out the isospin- $\frac{1}{2}$ and $\frac{3}{2}$ resonance contributions from these reaction amplitudes. As we know, the partial wave amplitudes $T_{l\pm}$ for the $\pi N \rightarrow \pi N$ reactions can be decomposed into the linear combinations of s -channel isospin amplitudes with the relations

$$T_{l\pm}(\pi^+ p \rightarrow \pi^+ p) = T_{l\pm}^{3/2}, \quad (13)$$

$$T_{l\pm}(\pi^- p \rightarrow \pi^- p) = +\frac{1}{3}(2T_{l\pm}^{1/2} + T_{l\pm}^{3/2}), \quad (14)$$

$$T_{l\pm}(\pi^- p \rightarrow \pi^0 n) = -\frac{\sqrt{2}}{3}(T_{l\pm}^{1/2} - T_{l\pm}^{3/2}), \quad (15)$$

where $T^{1/2}$ and $T^{3/2}$ correspond to the isospin- $\frac{1}{2}$, and $\frac{3}{2}$ resonance contributions, respectively. Using these relations, we can separate out s -channel isospin contributions from the $\pi N \rightarrow \pi N$ amplitudes.

In the $SU(6) \otimes O(3)$ symmetry limit, we have extracted the amplitudes for each s -channel resonances within $n \leq 2$ shell for the $\pi^+ p \rightarrow \pi^+ p, \pi^- p \rightarrow \pi^- p$ and $\pi^- p \rightarrow \pi^0 n$ processes. Our results are listed in Tables IV and V. Comparing the amplitudes of different resonances with each other, one can easily

TABLE I: Parameters.

Constituent quark mass	M_u	330 MeV
	M_d	330 MeV
	M_s	450 MeV
Harmonic oscillator parameter	α	400 MeV
degenerate masses of the $n = 1, 2$ shell resonances	M_1	1650 MeV
	M_2	1750 MeV
Parameters in t channel	$G_V a$	12
	$g_{SPPgSqq}$	65
	m_ρ	770 MeV
	m_σ	450 MeV
πNN coupling	$g_{\pi NN}$	13.48

find which states are the main contributors to the reactions in the $SU(6)\otimes O(3)$ symmetry limit.

Finally, the differential cross section $d\sigma/d\Omega$ and polarization P can be calculated by

$$\frac{d\sigma}{d\Omega} = \frac{(E_i + M_i)(E_f + M_f)}{64\pi^2 s(2M_i)(2M_f)} \frac{|\mathbf{q}|}{|\mathbf{k}|} \frac{1}{2} \times \sum_{\lambda_i, \lambda_f} |M_{\lambda_f, \lambda_i}|^2,$$

$$P = 2 \frac{\text{Im}[f(\theta)g(\theta)]}{|f(\theta)|^2 + |g(\theta)|^2}, \quad (16)$$

where $\lambda_i = \pm \frac{1}{2}$ and $\lambda_f = \pm \frac{1}{2}$ are the helicities of the initial and final state baryons respectively.

III. CALCULATION AND ANALYSIS

A. Parameters

In the calculation, we need four universal quark model parameters, i.e., the harmonic oscillator parameter α and constituent quark masses for the u , d , and s quarks. They are well determined in our previous works, thus, we fix them in our calculations. Their values are listed in Table I.

In the s and u channels, the quark- π -meson coupling is an overall parameter, which is related to the πNN coupling via the Goldberger-Treiman relation [63]

$$g_{\pi NN} = \frac{g_A M_N}{F_\pi}, \quad (17)$$

where g_A is the vector coupling for the π mesons. In the symmetrical quark model one can easily obtain $g_A = 5/3$ and $5\sqrt{2}/6$ for charged and neutral pions, respectively. F_π ($= f_\pi/\sqrt{2} \simeq 93$ MeV) is the pion-meson decay constant. It should be remarked that the πNN coupling is a well-determined number:

$$g_{\pi NN} = 13.48, \quad (18)$$

thus we fix it in our calculations.

In the t channel, there are two parameters, the coupling constants $G_V a$ from the ρ -meson exchange and $g_{SPPgSqq}$ from the σ -meson exchange. We determine these parameters by fitting the data, which are listed in Table I. It should be mentioned that the coupling constants $G_V a$ and $g_{SPPgSqq}$ bear about a 30% uncertainty.

In our framework, the s -channel resonance transition amplitude, O_R , is derived in the $SU(6)\otimes O(3)$ symmetry limit. In reality, the symmetry of $SU(6)\otimes O(3)$ is generally broken owing to some reasons. To accommodate the symmetry-breaking and hadronic dressing effects, following the idea of Ref. [47] we introduce a set coupling strength parameters, C_R , for each resonance amplitude,

$$O_R \rightarrow C_R O_R, \quad (19)$$

where C_R should be determined by fitting the data. The deviations of C_R from unity imply the $SU(6)\otimes O(3)$ symmetry breaking. The determined C_R values are listed in Table II. It is found that the C_R parameters for the $\Delta(1232)$ and $N(1440)$ resonances are notably larger than 1. Thus, the $SU(6)\otimes O(3)$ symmetry of these states is seriously broken by some effects, which will be discussed later in details.

Furthermore, the masses and widths for the s -channel resonances are important input parameters in the calculations. For the main resonances $\Delta(1232)P_{33}$ and $N(1440)P_{11}$, we vary their masses and widths in a proper range to better describe the data. To be consistent with our previous study, we take the masses and widths of $N(1535)S_{11}$ and $N(1520)D_{13}$ from [34], where the resonances parameters of $N(1535)S_{11}$ and $N(1520)D_{13}$ are well constrained. The other resonances have few effects on the reactions, thus, their masses and widths are taken from the PDG [4], or the constituent quark model predictions [54–56] if no experimental data are available. The masses and widths for some low-lying resonances have been listed in Table II. It is found that the mass and width for the $\Delta(1232)P_{33}$ are $M \simeq 1212$ MeV and $\Gamma \simeq 100$ MeV, respectively, which are consistent with those extracted from the neutral pion photoproduction processes in our previous work [36]. It should be emphasized that our extracted mass and width for the $\Delta(1232)P_{33}$ are quite close to the values of the pole parametrization from the PDG [4]. The reason is that, when we fit the data a constant resonance width Γ_R is used, which is similar to the pole parametrization. Furthermore, we find that the $N(1440)P_{11}$ resonance seems to favour a narrow width $\Gamma \simeq 200$ MeV, which is also comparable to the values of the pole parametrization from the PDG [4].

In the u channel, it is found that contributions from the $n \geq 1$ shell resonances are negligibly small and insensitive to their masses. Thus, the degenerate masses for the $n = 1, 2$ shell resonances are taken in our calculations. The values have been listed in Table I.

Finally, it should be pointed out that all the adjustable parameters are determined by globally fitting the measured differential cross sections, which are obtained from [38]. For the $\pi^+ p \rightarrow \pi^+ p$ reaction, we fit the differential cross sections in the incoming pion-meson momentum range $P_\pi = 260 \sim 420$ MeV/c, while for the $\pi^- p \rightarrow \pi^- p, \pi^0 n$ reactions, we fit the measured differential cross sections in the range $P_\pi = 260 \sim$

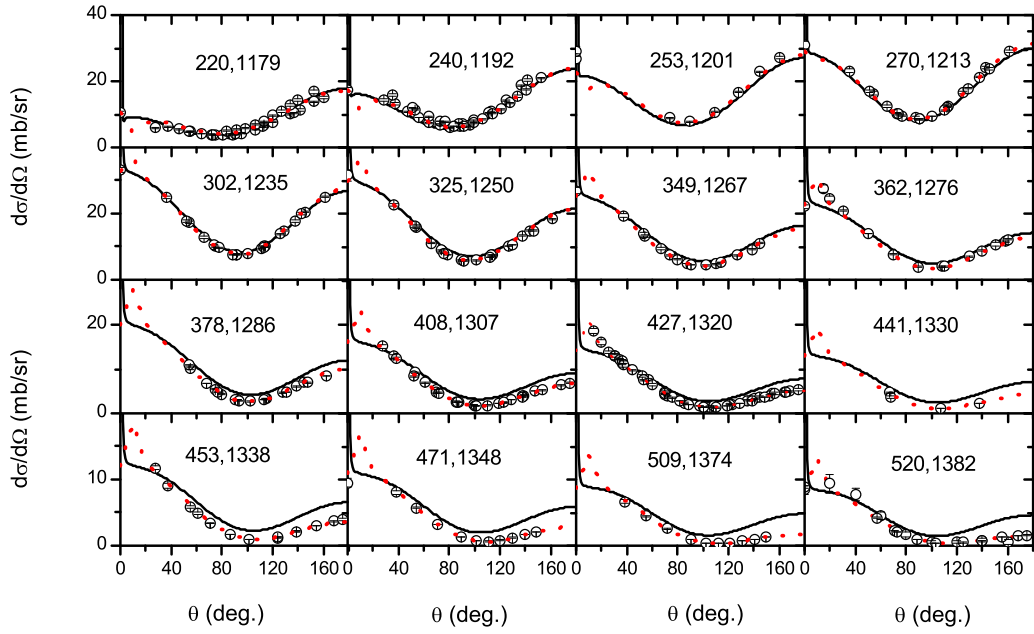


FIG. 1: Differential cross sections of the $\pi^+ p \rightarrow \pi^+ p$ reaction compared with the experimental data (open circles) from [64–68] and the solutions (dotted curves) from the GWU group [38]. The first and second numbers in each figure correspond to the incoming π momentum P_π (MeV) and the πN center-of-mass (c.m.) energy W (MeV), respectively.

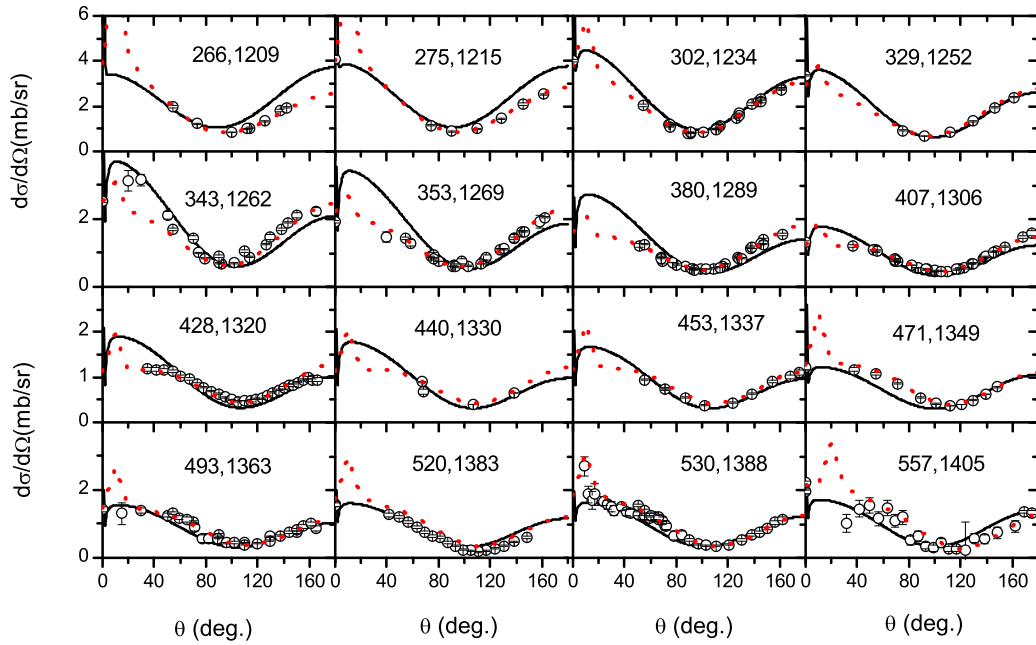


FIG. 2: Differential cross sections of the $\pi^- p \rightarrow \pi^- p$ reaction compared with the experimental data (open circles) from [64–68] and the solutions (dotted curves) from the GWU group [38]. The first and second numbers in each figure correspond to the incoming π momentum P_π (MeV) and the πN c.m. energy W (MeV), respectively.

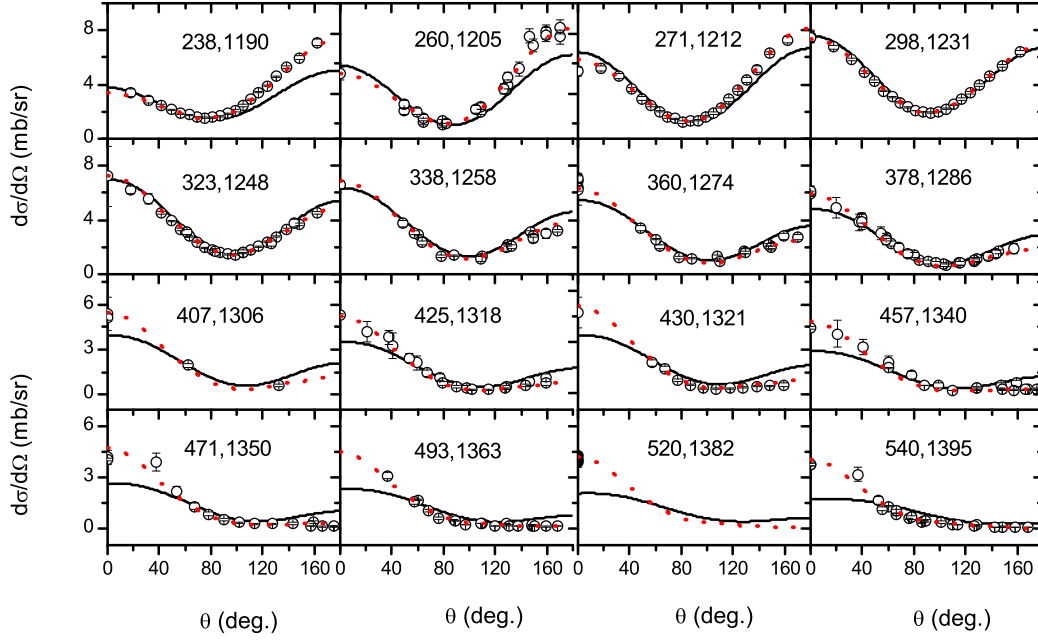


FIG. 3: Differential cross sections of the reaction $\pi^-p \rightarrow \pi^0n$ compared with the experimental data (open circles) from [69–74] and the solutions (dotted curves) from the GWU group [38]. The first and second numbers in each figure correspond to the incoming π momentum P_π (MeV) and the πN c.m. energy W (MeV), respectively.

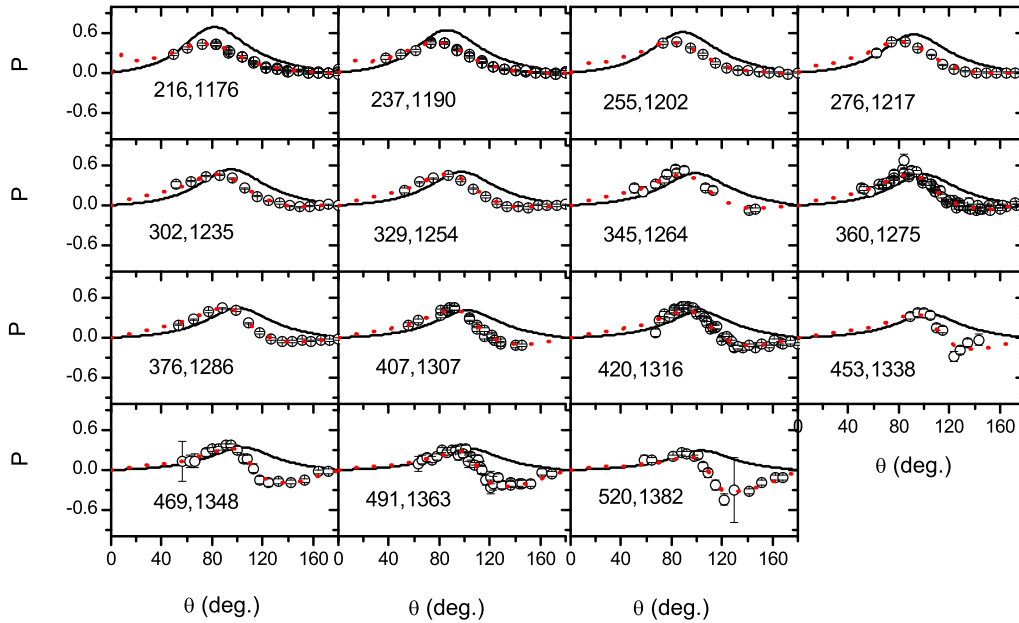


FIG. 4: Polarizations of the $\pi^+p \rightarrow \pi^+p$ reaction compared with experimental data (open circles) from [75–82] and the solutions (dotted curves) from the GWU group [38]. The first and second numbers in each figure correspond to the incoming π momentum P_π (MeV) and the πN c.m. energy W (MeV), respectively.

TABLE II: Masses M_R (MeV) and widths Γ_R (MeV) of s -channel intermediate states, and their C_R strength parameters.

Resonance	$\pi^+ p \rightarrow \pi^+ p$			$\pi^- p \rightarrow \pi^- p$			$\pi^- p \rightarrow \pi^0 n$		
	Γ_R	M_R	C_R	Γ_R	M_R	C_R	Γ_R	M_R	C_R
$N(938)P_{11}$	938	1.0	...	938	1.0
$\Delta(1232)P_{33}$	100^{+7}_{-4}	1212^{+3}_{-5}	$2.95^{+0.05}_{-0.20}$	100^{+7}_{-3}	1212^{+2}_{-5}	$3.00^{+0.05}_{-0.15}$	100^{+5}_{-2}	1210^{+2}_{-5}	$3.10^{+0.02}_{-0.15}$
$N(1440)P_{11}$	200^{+40}_{-35}	1400^{+40}_{-25}	23 ± 6	200^{+35}_{-20}	1400^{+40}_{-25}	23^{+6}_{-4}
$N(1535)S_{11}$	124	1524	1.0	124	1524	1.0
$\Delta(1620)S_{31}$	140	1630	1.0	140	1630	1.0	140	1630	1.0
$N(1650)S_{11}$	119	1670	1.0	119	1670	1.0
$\Delta(1700)D_{33}$	300	1745	1.0	300	1745	1.0	300	1745	1.0
$N(1520)D_{13}$	125	1515	1.0	125	1515	1.0
$N(1700)D_{13}$	150	1700	1.0	150	1700	1.0
$N(1675)D_{15}$	150	1675	1.0	150	1675	1.0

TABLE III: Reduced χ^2 per data point of the full model and that with one resonance or one background switched off obtained in a fit of the measured differential cross sections of the $\pi^+ p \rightarrow \pi^+ p$ and $\pi^- p \rightarrow \pi^- p, \pi^0 n$ reactions. Their corresponding χ^2 s are labeled with $\chi^2_{\pi^+ p}, \chi^2_{\pi^- p}$ and $\chi^2_{\pi^0 n}$, respectively.

	full model	n pole	$\Delta(1232)P_{33}$	$N(1535)S_{11}$	$N(1520)D_{13}$	$N(1440)P_{11}$	u channel	t channel
$\chi^2_{\pi^+ p}$	3.21	...	74.84	5.10	7.71
$\chi^2_{\pi^- p}$	2.48	9.89	59.40	3.29	2.49	4.55	8.36	4.33
$\chi^2_{\pi^0 n}$	3.60	5.70	147.21	8.15	3.87	4.80	19.14	7.77

540 MeV/c. The data sets used in our fits are shown in Figs. 1, 2 and 3. The reduced χ^2 s per data point obtained in our fits are listed in Table II. To clearly see the role of one component in the reactions, the χ^2 s with one resonance or one background switched off are also given in the Table III.

B. $\pi^+ p \rightarrow \pi^+ p$

The $\pi^+ p \rightarrow \pi^+ p$ process provides us a rather clear channel to study the Δ resonances, because only the isospin 3/2 resonances contribute here for the isospin selection rule. The low-lying Δ resonances classified in the quark model are listed in Table IV. From the table we can see that in a rather wide πN center-of-mass (c.m.) energy range $W < 1.6$ GeV, only the $\Delta(1232)P_{33}$ resonance lies. The higher resonances are the S -wave state $\Delta(1620)S_{31}$ and the D -wave state $\Delta(1700)D_{33}$, which may mainly contribute to the reaction in the higher energy range $W > 1.5$ GeV. Thus, the description of the $\pi^+ p \rightarrow \pi^+ p$ reaction in the low energy region becomes relatively simple.

The chiral quark model allows us study the $\pi^+ p \rightarrow \pi^+ p$ reaction from the $\Delta(1232)$ resonance region up to $W \simeq 1.4$ GeV. Our fits of the differential cross sections and polarizations compared with the data are shown in Figs. 1 and 4, respectively. From these figures, it is found that our fits are in a global agreement with the experimental data in the c.m. energy range $W \simeq 1.2 - 1.4$ GeV, although in our calculations the polarizations are overestimated slightly at the backward angles, and the cross sections are overestimated slightly in the

region $W > 1.3$ GeV. New precise measurements with a good angle coverage are hoped to be carried out in the future. For the limitations of the present model, our study cannot cover the higher energy region $W > 1.4$ GeV.

To clearly understand the reaction mechanism of $\pi^+ p \rightarrow \pi^+ p$, we show the main contributors one by one in Fig. 5. It is found that the interferences between the $\Delta(1232)P_{33}$ resonance and the backgrounds of the u and t channels can roughly explain the $\pi^+ p \rightarrow \pi^+ p$ reaction up to $W \simeq 1.4$ GeV. The Coulomb interactions may play an obvious role at the extremely forward angles. Slight effects from the contact term can also be seen at the forward and backward angles. The behavior of the contact term is similar to that of the t channel. No obvious effects of the higher resonances, such as $\Delta(1620)S_{31}$ and $\Delta(1700)D_{33}$, are found in the low energy region what we consider.

The cross sections around $W = 1.2$ GeV are sensitive to the mass and width of $\Delta(1232)P_{33}$, which provide us a good place to constrain the resonance parameters of $\Delta(1232)P_{33}$. By fitting the measured total cross section with a momentum independent width (see Fig. 6), we obtain that the mass and width of $\Delta(1232)P_{33}$ are $M \simeq 1212$ MeV and $\Gamma \simeq 100$ MeV, respectively, with a uncertainty of several MeV. These determined mass and width of $\Delta(1232)P_{33}$ are consistent with our recent analysis of the pions photoproduction reactions [36], and also are quite close to the values of the pole parametrization from the PDG [4].

Finally, it should be pointed out that to obtain a better description of the data, we should enhance the $\Delta(1232)P_{33}$ contribution with a factor of $C_\Delta \simeq 3.0$, which indicates that the

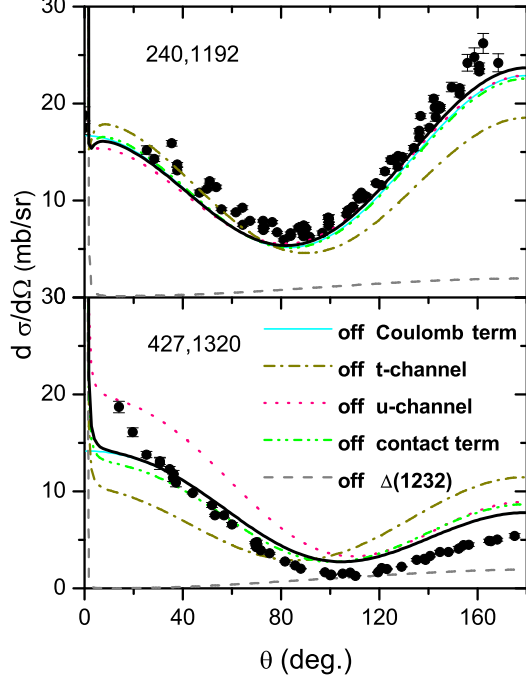


FIG. 5: Effects of the main contributors on the differential cross sections of the reaction $\pi^+ p \rightarrow \pi^+ p$ at two energy points $P_\pi = 240, 427$ MeV/c. The experimental data are taken from [64–66]. The bold solid curves correspond to the full model result. The predictions by switching off the contributions from $\Delta(1232)P_{33}$, u - and t -channel backgrounds are indicated explicitly by the legend in the figures.

$\Delta(1232)N\pi$ coupling may be underestimated by a factor of $\sim \sqrt{3}$ in the $SU(6) \otimes O(3)$ symmetry limit. This underestimation is also found in the pions photoproduction reactions [36] and the strong decays of $\Delta(1232)P_{33}$ [86]. The $\Delta(1232)P_{33}$ might not be a pure three-quark state [87–92], some other contributions, such as meson-baryon component, may alter the $\Delta(1232)N\pi$ coupling.

As a whole, from the $\Delta(1232)$ resonance region up to the $N(1440)$ resonance region, the $\pi^+ p$ elastic scattering can be reasonably understood with the interferences between the $\Delta(1232)P_{33}$ resonance and the backgrounds of the u and t channels. The extracted mass and width of $\Delta(1232)P_{33}$ are quite close to the values of the pole parametrization [4]. The large $\Delta(1232)N\pi$ coupling out of the quark model prediction may indicate that $\Delta(1232)P_{33}$ may not be a pure three-quark state.

C. $\pi^- p \rightarrow \pi^- p, \pi^0 n$

Both the isospin-1/2 and -3/2 resonances contribute to the $\pi^- p \rightarrow \pi^- p, \pi^0 n$ reactions. From the spectrum classified in the quark model (see Table IV), we find that only the $\Delta(1232)P_{33}$ and $N(1440)P_{11}$ resonances lie within the $N(1440)P_{11}$ resonance region. The higher resonances

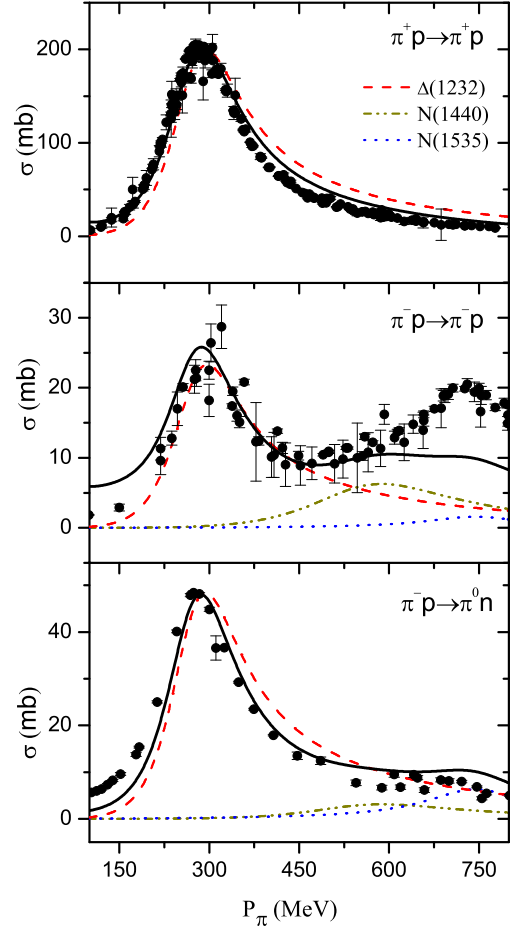


FIG. 6: Predicted total cross sections of the reaction $\pi^+ p \rightarrow \pi^+ p$ and $\pi^- p \rightarrow \pi^- p, \pi^0 n$ compared with experimental data. The data for the $\pi^+ p \rightarrow \pi^+ p$ reactions are obtained from the PDG [4], and the data of $\pi^- p \rightarrow \pi^0 n$ are taken from the Refs. [69–71, 83–85]. The bold solid curves correspond to the full model result. In the figure, exclusive cross sections for $\Delta(1232)P_{33}$, $N(1535)S_{11}$, and $N(1440)P_{11}$ are indicated explicitly by the legends.

$N(1535, 1650)S_{11}$, $\Delta(1620)S_{31}$, $N(1520)D_{13}$ and $\Delta(1700)D_{33}$ are far from the $N(1440)P_{11}$ resonance region, thus, their affects on these reactions should be small within this energy region. In this sense, the $\pi^- p \rightarrow \pi^- p, \pi^0 n$ reactions might be good places to study the properties of the $\Delta(1232)P_{33}$ and $N(1440)P_{11}$ resonances.

Based on our good understanding of $\pi^+ p \rightarrow \pi^+ p$, we further study the $\pi^- p \rightarrow \pi^- p, \pi^0 n$ reactions. Our fits of the differential cross sections, total cross sections, and polarizations compared with the data are shown in Figs. 2, 3, 6-8. From these figures, it is found that the experimental data from $\Delta(1232)$ resonance region the up to the $N(1440)$ resonance region are reasonably described within the chiral quark model. It should be mentioned that there are remaining discrepancies

in the polarizations of $\pi^- p \rightarrow \pi^- p$ below $W = 1.3$ GeV. To gain more knowledge of these reactions, new precise measurements of the polarizations with a good angle and energy coverage is hoped to be carried out in the future.

To clearly understand the low energy reactions $\pi^- p \rightarrow \pi^- p, \pi^0 n$, we show the main contributions to the differential cross sections and polarizations in Figs. 10 and 11, respectively. From these figures, it is found that besides $\Delta(1232)P_{33}$, the Roper $N(1440)P_{11}$ plays a crucial role in the $\pi^- p \rightarrow \pi^- p, \pi^0 n$ reactions. Switching off their contributions, we find that the differential cross sections and polarizations have a notable change at both forward and backward angles. It should be emphasized that a confirmed role of $N(1440)P_{11}$ can be more obviously seen from the polarizations. Slight contributions from the $N(1535)S_{11}$ and $D(1520)D_{13}$ resonances can extend to the $N(1440)$ resonance region as well, for simplicity, we do not show them in the figures. No obvious effects of the higher resonances, such as $\Delta(1620)S_{31}$, $\Delta(1700)D_{33}$, $D(1700)D_{13}$, and $D(1675)D_{15}$ in the low energy regions. The backgrounds from the s -channel nucleon pole, u and t channels play important roles in the reactions. The Coulomb interactions may play an obvious role at the extremely forward angles. Slight effects from the contact term can also be seen at the forward and backward angles.

Furthermore, to better understand the properties of the $\Delta(1232)P_{33}$ and $N(1440)P_{11}$ resonances, we also show our fits of the P_{11} and P_{33} amplitudes to the solution WI08 [10] from the GWU group [38] in fig. 9. Our results show a good agreement with the solution WI08. Beyond the mass threshold of $N(1440)P_{11}$, although the real part of the P_{11} amplitude is overestimated in our quark model, its tendency is similar to the solution WI08. It should be mentioned that in the higher energy region $W \simeq 1.4$ GeV, our quark model begins to lose its prediction ability, thus, our extracted properties of $N(1440)P_{11}$ may be less reliable than those of $\Delta(1232)P_{33}$.

In the $\pi^- p \rightarrow \pi^- p, \pi^0 n$ reactions, to obtain a good description of the data we also need enhance the contribution of $\Delta(1232)P_{33}$ from the symmetric quark model with a factor of $C_\Delta \simeq 3.0$. The extracted mass and width of $\Delta(1232)P_{33}$ from these two reactions are consistent with those from the $\pi^+ p \rightarrow \pi^+ p$ reaction. At the mass threshold of $\Delta(1232)P_{33}$, our extracted ratios of the total cross sections between these three πN reactions

$$\begin{aligned} \sigma(\pi^+ p \rightarrow \pi^+ p) : \sigma(\pi^- p \rightarrow \pi^- p) : \sigma(\pi^- p \rightarrow \pi^0 n) \\ \simeq 205 : 25 : 48, \end{aligned} \quad (20)$$

are quite close to the theoretical ratios $9 : 1 : 2$, which indicates that the isospin symmetry well holds in these low energy πN reactions.

Finally, it should be emphasized that confirmed roles of $N(1440)P_{11}$ have been seen in the $\pi^- p \rightarrow \pi^- p, \pi^0 n$ reactions, which provide us a good opportunity to extract the properties of $N(1440)P_{11}$. From the data of the $\pi^- p \rightarrow \pi^- p, \pi^0 n$ reactions, we extract the mass and width of $N(1440)P_{11}$, $M \simeq 1400$ MeV and $\Gamma \simeq 200$ MeV, which are close to those extracted from the pole parametrization [4]. Furthermore, it should be mentioned that to well describe the data we need

enhance the contribution of the $N(1440)P_{11}$ from the symmetric quark model with a rather large factor $C_{N(1440)} \simeq 23$, i.e., the $N(1440)N\pi$ coupling is a factor ~ 4.8 larger than the prediction with the simple three-quark model, which was also found by analyzing the strong decays of $N(1440)P_{11}$ in Refs. [102, 103]. The unexpected large $N(1440)N\pi$ coupling indicates the exotic nature of the $N(1440)P_{11}$ resonance. About the unusual properties of $N(1440)$, there are many discussions in the literature [11, 26, 104–114].

As a whole, besides the $\Delta(1232)P_{33}$ resonance, confirmed evidence of the $N(1440)P_{11}$ resonance is found in the polarizations of the $\pi^- p \rightarrow \pi^- p, \pi^0 n$ reactions. The couplings of the $\Delta(1232)N\pi$ and $N(1440)N\pi$ predicted from the simple three-quark model are about 1.7 and 4.8 times smaller than the values extracted from the experimental data, respectively, which indicates that the $\Delta(1232)P_{33}$ and $N(1440)P_{11}$ resonances cannot be pure three-quark states. Finally, it should be mentioned that the s -channel nucleon pole, u - and t -channel backgrounds play important roles in the reactions.

IV. SUMMARY

In this work, a combined study of the $\pi^+ p \rightarrow \pi^+ p, \pi^- p \rightarrow \pi^- p$ and $\pi^- p \rightarrow \pi^0 n$ reactions have been carried out within a chiral quark model. Our results show a good global agreement with the data within the $N(1440)$ resonance region.

In these reactions, the resonance properties of $\Delta(1232)P_{33}$ are constrained. By fitting the data with a momentum independent width, we obtain the mass and width of $\Delta(1232)P_{33}$ are $M \simeq 1212$ MeV and $\Gamma \simeq 100$ MeV, which are consistent with our recent analysis of the pions photoproduction reactions [36], and are quite close to the values determined with the pole parametrization [4]. The $\Delta(1232)N\pi$ coupling from the quark model is about a factor of ~ 1.7 smaller than that extracted from the data. Some exotic components, such as the meson-baryon component, may alter the $\Delta(1232)N\pi$ coupling, which should be studied further.

Confirmed roles of $N(1440)P_{11}$ resonance are found in both the $\pi^- p \rightarrow \pi^- p$ and $\pi^- p \rightarrow \pi^0 n$ reactions. The $N(1440)P_{11}$ has notable contributions to the polarizations, although no obvious effects can be seen in the total cross sections. The extracted mass and width for $N(1440)P_{11}$ are $M \simeq 1400$ MeV and $\Gamma \simeq 200$ MeV, respectively, which are close to the values determined with the pole parametrization [4]. The $N(1440)N\pi$ coupling extracted from the data is a factor of ~ 4.8 larger than the symmetric quark model prediction. The unexpected large $N(1440)N\pi$ coupling suggests the uncommon properties of the $N(1440)P_{11}$ resonance.

Starting from the incoming π -meson momentum $P_\pi \simeq 440$ MeV/c, slight contributions of $N(1535)S_{11}$ and $N(1520)D_{13}$ are seen in both the $\pi^- p \rightarrow \pi^- p$ and $\pi^- p \rightarrow \pi^0 n$ reactions. The backgrounds play remarkable roles in these three strong interaction processes. The t - and u -channel backgrounds have notable contributions to the $\pi^+ p \rightarrow \pi^+ p$ reactions. While in the $\pi^- p \rightarrow \pi^- p, \pi^0 n$ reactions, the s -channel nucleon pole and t - and u -channel backgrounds play an important role.

Finally, it should be pointed out that with present model

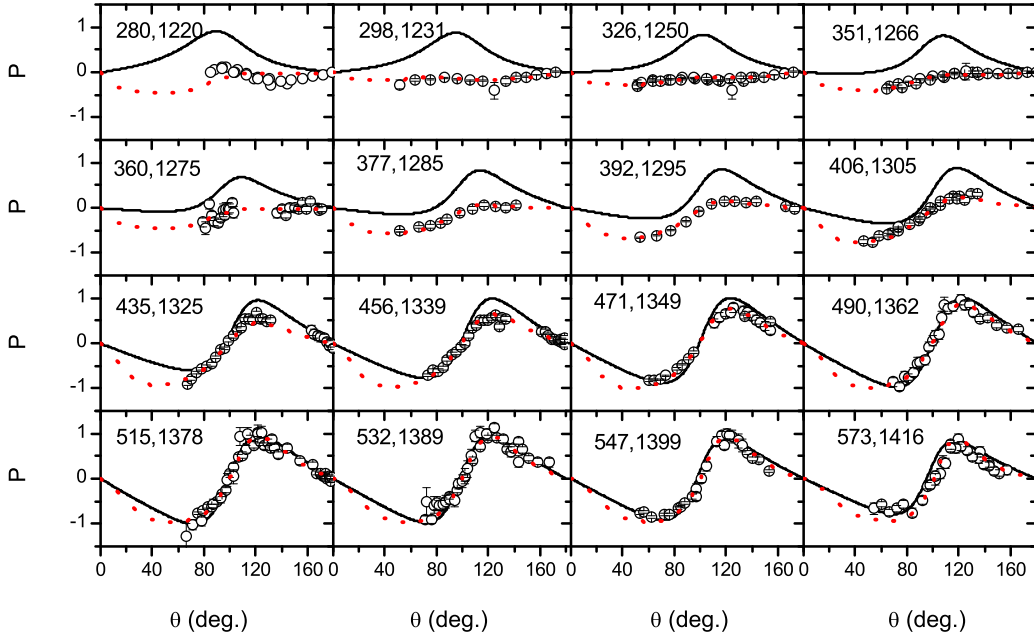


FIG. 7: Polarizations of the $\pi^- p \rightarrow \pi^- p$ reaction compared with experimental data (open circles) from [75, 76, 93–95] and the solutions (dotted curves) from the GWU group [38]. The first and second numbers in each figure correspond to the incoming π momentum P_π (MeV) and the πN c.m. energy W (MeV), respectively.

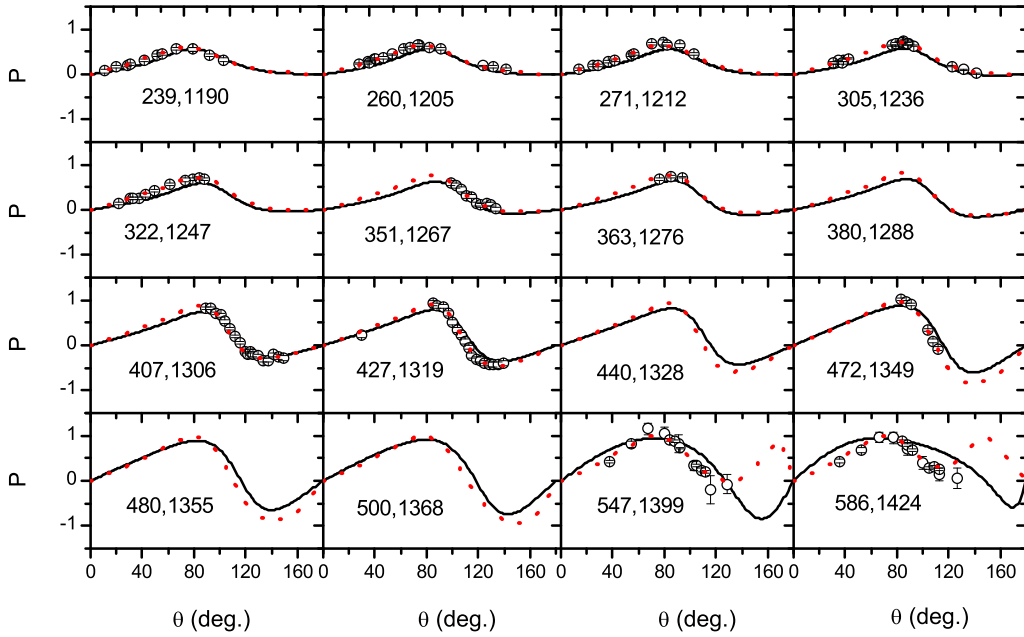


FIG. 8: Polarizations of the $\pi^- p \rightarrow \pi^0 n$ reaction compared with the experimental data (open circles) from [74, 94, 96–98] and the solutions (dotted curves) from the GWU group [38]. The first and second numbers in each figure correspond to the incoming π momentum P_π (MeV) and the πN c.m. energy W (MeV), respectively.

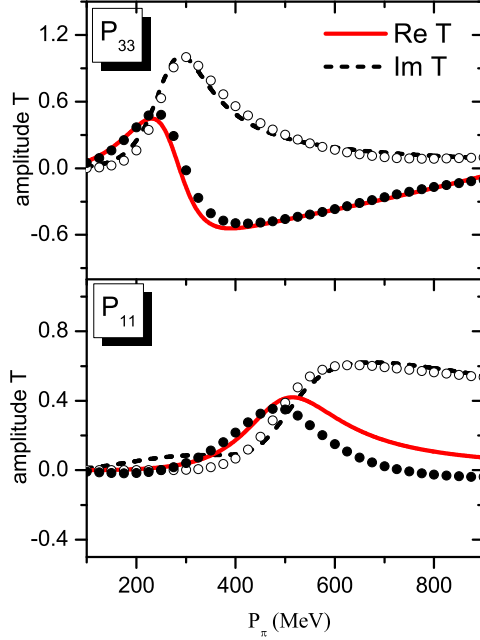


FIG. 9: The πN partial amplitudes of P_{33} and P_{11} . Solid (dashed) curves give the real (imaginary) parts of amplitudes extracted from our quark model. The filled (open) circles stand for the real (imaginary) parts (solution WI08 [10]) extracted by the GWU group [38].

we cannot deliver higher accuracy descriptions of the data because there are only a few adjustable parameters based on the $SU(6) \otimes O(3)$ symmetry, and all of the interactions are limited at the tree level. Furthermore, our present study is difficult to cover the whole $N(1440)P_{11}$ resonance region, thus, the extracted properties of $N(1440)P_{11}$ may bear a large uncertainty although confirmed roles of $N(1440)P_{11}$ are found in the polarizations. To uncover the uncommon nature of $N(1440)P_{11}$, new precise measurements of the polarizations with a good angle and energy coverage are expected to be carried out in the future.

Acknowledgments

We are grateful for useful discussions and suggestions from Qiang Zhao, Fei Huang, Jia-Jun Wu, Ju-Jun Xie and Xu Cao. This work is partly supported by the National Natural Science Foundation of China (Grants No. 11075051 and No. 11375061), the Hunan Provincial Natural Science Foundation (Grant No. 13JJ1018), and the Hunan Provincial Innovation Foundation for Postgraduate.

-
- [1] V. Crede and W. Roberts, Progress towards understanding baryon resonances, Rept. Prog. Phys. **76**, 076301 (2013).
- [2] E. Klempt and J.M. Richard, Baryon spectroscopy, Rev. Mod. Phys. **82**, 1095 (2010).
- [3] W. J. Briscoe, M. Döring, H. Haberzettl, D. M. Manley, M. Naruki, I. I. Strakovsky and E. S. Swanson, Physics opportunities with meson beams, Eur. Phys. J. A **51**, 129 (2015).
- [4] K. A. Olive *et al.* [Particle Data Group Collaboration], Review of Particle Physics, Chin. Phys. C **38**, 090001 (2014).
- [5] R. Koch and E. Pietarinen, Low-energy πN partial wave analysis, Nucl. Phys. A **336**, 331 (1980).
- [6] R. E. Cutkosky, R. E. Hendrick, J. W. Alcock, Y. A. Chao, R. G. Lipes, J. C. Sandusky and R. L. Kelly, Pion-nucleon partial wave analysis, Phys. Rev. D **20**, 2804 (1979).
- [7] R. E. Cutkosky, C. P. Forsyth, R. E. Hendrick and R. L. Kelly, Pion-nucleon partial wave amplitudes, Phys. Rev. D **20**, 2839 (1979).
- [8] R. A. Arndt, J. M. Ford and L. D. Roper, Pion-nucleon partial wave analysis to 1100 MeV, Phys. Rev. D **32**, 1085 (1985).
- [9] R. E. Cutkosky and S. Wang, Poles of the $\pi N P_{11}$ partial wave amplitude, Phys. Rev. D **42**, 235 (1990).
- [10] R. A. Arndt, W. J. Briscoe, I. I. Strakovsky and R. L. Workman, Extended partial-wave analysis of πN scattering data, Phys. Rev. C **74**, 045205 (2006).
- [11] O. Krehl, C. Hanhart, S. Krewald and J. Speth, What is the structure of the Roper resonance?, Phys. Rev. C **62**, 025207 (2000).
- [12] M. Doring, C. Hanhart, F. Huang, S. Krewald and U.-G. Meissner, Analytic properties of the scattering amplitude and resonances parameters in a meson exchange model, Nucl. Phys. A **829**, 170 (2009).
- [13] D. Ronchen *et al.*, Coupled-channel dynamics in the reactions $\pi N \rightarrow \pi N, \eta N, K\Lambda, K\Sigma$, Eur. Phys. J. A **49**, 44 (2013).
- [14] H. Kamano, S. X. Nakamura, T.-S. H. Lee and T. Sato, Extraction of P_{11} resonances from πN data, Phys. Rev. C **81**, 065207 (2010).
- [15] A. Matsuyama, T. Sato and T.-S. H. Lee, Dynamical coupled-channel model of meson production reactions in the nucleon resonance region, Phys. Rept. **439**, 193 (2007).
- [16] B. Julia-Diaz, T.-S. H. Lee, A. Matsuyama and T. Sato, Dynamical coupled-channel model of πN scattering in the $W \leq 2$ GeV nucleon resonance region, Phys. Rev. C **76**, 065201 (2007).
- [17] H. Kamano, S. X. Nakamura, T.-S. H. Lee and T. Sato, Nucleon resonances within a dynamical coupled-channels model of πN and γN reactions, Phys. Rev. C **88**, 035209 (2013).
- [18] G. Penner and U. Mosel, Vector meson production and nucleon resonance analysis in a coupled channel approach for energies $m_N < \sqrt{s} < 2$ GeV. I. Pion induced results and hadronic parameters, Phys. Rev. C **66**, 055211 (2002).
- [19] V. Shklyar, H. Lenske, U. Mosel and G. Penner, Coupled-channel analysis of the omega-meson production in πN and γN reactions for c.m. energies up to 2 GeV, Phys. Rev. C **71**, 055206 (2005) Erratum: [Phys. Rev. C **72**, 019903 (2005)].
- [20] A. Anisovich, E. Klempt, A. Sarantsev and U. Thoma, Partial wave decomposition of pion and photoproduction amplitudes,

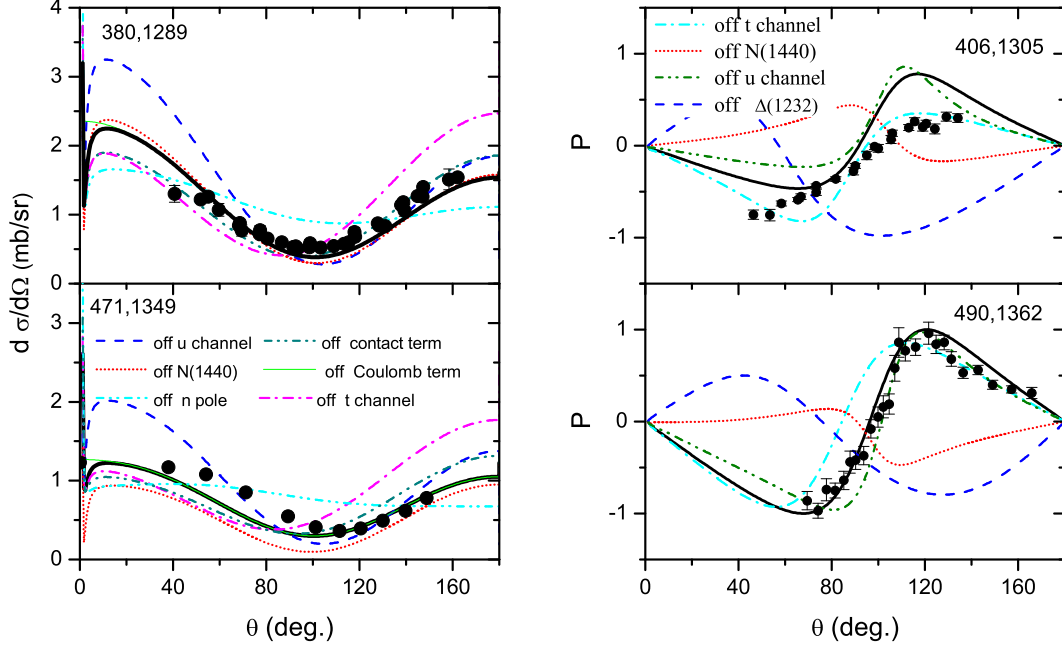


FIG. 10: Effects of the main contributors on the differential cross sections (left side) and polarizations (right side) of the reaction $\pi^- p \rightarrow \pi^- p$. The experimental data are taken from [64–68, 76]. The bold solid curves correspond to the full model result. The results by switching off the one of the main contributors in the resonances and non-resonance backgrounds are indicated explicitly by the legend in the figures. The first and second numbers in each figure correspond to the incoming π momentum P_π (MeV) and the πN c.m. energy W (MeV), respectively.

- Eur. Phys. J. A **24**, 111 (2005).
- [21] A. V. Anisovich, E. Klempt, V. A. Nikonov, A. V. Sarantsev and U. Thoma, P-wave excited baryons from pion- and photo-induced hyperon production, Eur. Phys. J. A **47**, 27 (2011).
- [22] S. Ceci, A. Svarc and B. Zauner, The $\pi N \rightarrow \eta N$ data demand the existence of $N(1710)P_{11}$ resonance reducing the 1700 MeV continuum ambiguity, Phys. Rev. Lett. **97**, 062002 (2006).
- [23] A. Švarc, M. Hadžimehmedović, H. Osmanović, J. Stahov and R. L. Workman, Pole structure from energy-dependent and single-energy fits to GWU-SAID N elastic scattering data, Phys. Rev. C **91**, 015207 (2015).
- [24] A. Švarc, M. Hadžimehmedović, R. Omerović, H. Osmanović and J. Stahov, Poles of Karlsruhe-Helsinki KH80 and KA84 solutions extracted by using the Laurent-Pietarinen method, Phys. Rev. C **89**, 045205 (2014).
- [25] J. J. Wu, H. Kamano, T.-S. H. Lee, D. B. Leinweber and A. W. Thomas, Nucleon resonance structure in the finite volume of lattice QCD, arXiv:1611.05970 [hep-lat].
- [26] N. Suzuki, B. Julia-Diaz, H. Kamano, T.-S. H. Lee, A. Matsuyama and T. Sato, Disentangling the dynamical origin of P_{11} nucleon resonances, Phys. Rev. Lett. **104**, 042302 (2010).
- [27] G. Y. Chen, S. S. Kamalov, S. N. Yang, D. Drechsel and L. Tiator, Nucleon resonances in πN scattering up to energies $\sqrt{s} < 2$ GeV, Phys. Rev. C **76**, 035206 (2007).
- [28] J. Segovia, B. El-Bennich, E. Rojas, I. C. Cloet, C. D. Roberts, S. S. Xu and H. S. Zong, Completing the picture of the Roper resonance, Phys. Rev. Lett. **115**, no. 17, 171801 (2015).
- [29] N. Kaiser, P. B. Siegel and W. Weise, Chiral dynamics and the $S_{11}(1535)$ nucleon resonance, Phys. Lett. B **362**, 23 (1995).
- [30] J. Nieves and E. Ruiz Arriola, The S_{11} - $N(1535)$ and $-N(1650)$ resonances in meson baryon unitarized coupled channel chiral perturbation theory, Phys. Rev. D **64**, 116008 (2001).
- [31] T. Inoue, E. Oset and M. J. Vicente Vacas, Chiral unitary approach to S wave meson baryon scattering in the strangeness $S = 0$ sector, Phys. Rev. C **65**, 035204 (2002).
- [32] M. Doring, E. Oset and B. S. Zou, The role of the $N^*(1535)$ resonance and the $\pi^- p \rightarrow KY$ amplitudes in the OZI forbidden $\pi N \rightarrow \phi N$ reaction, Phys. Rev. C **78**, 025207 (2008).
- [33] M. Doring and K. Nakayama, The phase and pole structure of the $N^*(1535)$ in $\pi N \rightarrow \pi N$ and $\gamma N \rightarrow \pi N$, Eur. Phys. J. A **43**, 83 (2010).
- [34] L. Y. Xiao, F. Ouyang, Kai-Lei Wang and X. H. Zhong, Combined analysis of the $\pi^- p \rightarrow K^0 \Lambda$, ηn reactions in a chiral quark model, Phys. Rev. C **94**, 035202 (2016).
- [35] X. H. Zhong, Q. Zhao, J. He and B. Saghai, Study of $\pi^- p \rightarrow \eta n$ at low energies in a chiral constituent quark model, Phys. Rev. C **76**, 065205 (2007).
- [36] L. Y. Xiao, X. Cao and X. H. Zhong, Neutral pion photoproduction on the nucleon in a chiral quark model, Phys. Rev. C **92**, 035202 (2015).
- [37] X. H. Zhong and Q. Zhao, η photoproduction on the quasi-free nucleons in the chiral quark model, Phys. Rev. C **84**, 045207 (2011).
- [38] INS Data Analysis Center, George Washington University, <http://gwdac.phys.gwu.edu>.
- [39] Q. Zhao, Chiral quark model approach for the study of baryon resonances, Prog. Theor. Phys. Suppl. **186**, 253 (2010).
- [40] Z. P. Li, H. X. Ye and M. H. Lu, A unified approach to pseudoscalar meson photoproductions off nucleons in the quark model, Phys. Rev. C **56**, 1099 (1997).
- [41] X. H. Zhong and Q. Zhao, η' photoproduction on the nucleons

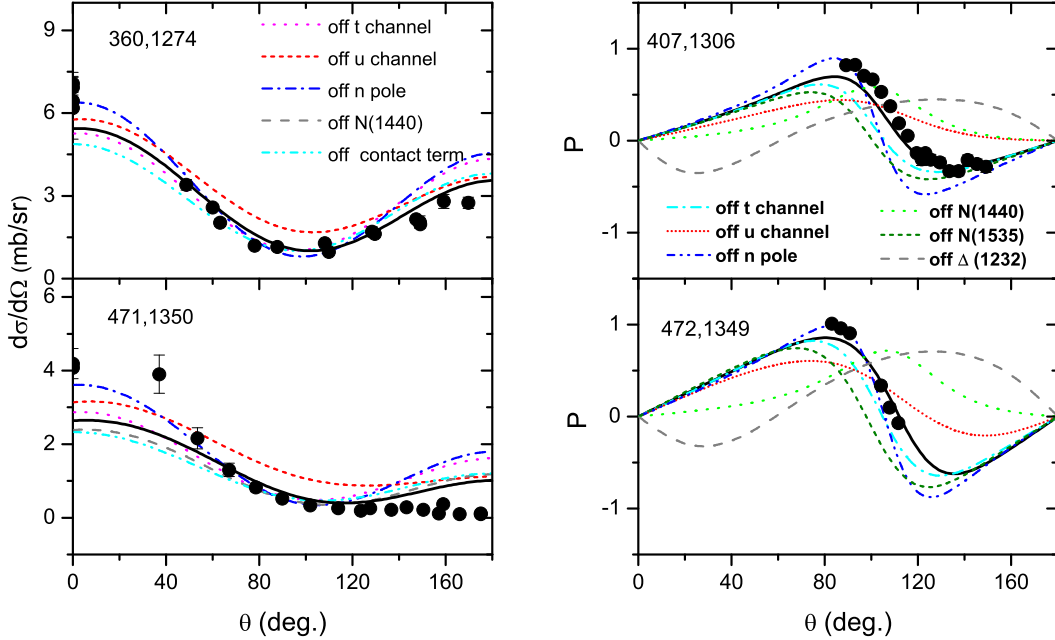


FIG. 11: Effects of the main contributors on the differential cross sections (left side) and polarizations (right side) of the reaction $\pi^- p \rightarrow \pi^0 n$. The experimental data are taken from [69, 73, 99–101]. The bold solid curves correspond to the full model result. The predictions by switching off the one of the main contributors in the resonances and non-resonance backgrounds are indicated explicitly by the legend in the figures. The first and second numbers in each figure correspond to the incoming π momentum P_π (MeV) and the πN c.m. energy W (MeV), respectively.

- in the quark model, Phys. Rev. C **84**, 065204 (2011).
- [42] Z. P. Li, The threshold pion photoproduction of nucleons in the chiral quark model, Phys. Rev. D **50**, 5639 (1994).
- [43] Z. P. Li, The Kaon photoproduction of nucleons in the chiral quark model, Phys. Rev. C **52**, 1648 (1995).
- [44] Z. P. Li, The η photoproduction of nucleons and the structure of the resonance $S_{11}(1535)$ in the quark model, Phys. Rev. D **52**, 4961 (1995).
- [45] Q. Zhao, J. S. Al-Khalili, Z. P. Li and R. L. Workman, Pion photoproduction on the nucleon in the quark model, Phys. Rev. C **65**, 065204 (2002).
- [46] Z. P. Li and B. Saghai, Study of the baryon resonances structure via eta photoproduction, Nucl. Phys. A **644**, 345 (1998).
- [47] B. Saghai and Z. P. Li, Quark model study of the eta photoproduction: Evidence for a new S_{11} resonance?, Eur. Phys. J. A **11**, 217 (2001).
- [48] Q. Zhao, B. Saghai and Z. P. Li, Quark model approach to the eta meson electroproduction on the proton, J. Phys. G **28**, 1293 (2002).
- [49] J. He, B. Saghai and Z. P. Li, Study of η photoproduction on the proton in a chiral constituent quark approach via one-gluon-exchange model, Phys. Rev. C **78**, 035204 (2008).
- [50] J. He and B. Saghai, Combined study of $\gamma p \rightarrow \eta p$ and $\pi i^- p \rightarrow \eta n$ in a chiral constituent quark approach, Phys. Rev. C **80**, 015207 (2009).
- [51] L. Y. Xiao and X. H. Zhong, Low-energy $K^- p \rightarrow \Lambda \eta$ reaction and the negative parity Λ resonances, Phys. Rev. C **88**, 065201 (2013).
- [52] X. H. Zhong and Q. Zhao, The $K^- p \rightarrow \Sigma^0 \pi^0$ reaction at low energies in a chiral quark model, Phys. Rev. C **79**, 045202 (2009).
- [53] X. H. Zhong and Q. Zhao, Low energy reactions $K^- p \rightarrow \Sigma^0 \pi^0$, $\Lambda \pi^0$, $\bar{K}^0 n$ and the strangeness $S = -1$ hyperons, Phys. Rev. C **88**, 015208 (2013).
- [54] N. Isgur and G. Karl, P wave baryons in the quark model, Phys. Rev. D **18**, 4187 (1978).
- [55] N. Isgur and G. Karl, Hyperfine interactions in negative parity baryons, Phys. Lett. B **72**, 109 (1977).
- [56] N. Isgur and G. Karl, Positive parity excited baryons in a quark model with hyperfine interactions, Phys. Rev. D **19**, 2653 (1979) Erratum: [Phys. Rev. D **23**, 817 (1981)].
- [57] M. F. M. Lutz and E. E. Kolomeitsev, Relativistic chiral SU(3) symmetry, large N_c sum rules and meson baryon scattering, Nucl. Phys. A **700**, 193 (2002).
- [58] B. Tromborg, S. Waldenstrom and I. Overbo, Electromagnetic Corrections to πN Scattering, Phys. Rev. D **15**, 725 (1977).
- [59] A. Gashi, E. Matsinos, G. C. Oades, G. Rasche and W. S. Woolcock, Electromagnetic corrections to the hadronic phase shifts in low-energy $\pi^+ p$ elastic scattering, Nucl. Phys. A **686**, 447 (2001).
- [60] A. Gashi, E. Matsinos, G. C. Oades, G. Rasche and W. S. Woolcock, Electromagnetic corrections for the analysis of low-energy $\pi^- p$ scattering data, Nucl. Phys. A **686**, 463 (2001).
- [61] E. Matsinos, W. S. Woolcock, G. C. Oades, G. Rasche and A. Gashi, Phase-shift analysis of low-energy $\pi^\pm p$ elastic-scattering data, Nucl. Phys. A **778**, 95 (2006).
- [62] J. Hamilton and W. S. Woolcock, Determination of pion-

TABLE IV: The s -channel resonance amplitudes within $n=2$ shell for the $\pi^+ p \rightarrow \pi^+ p$, $\pi^- p \rightarrow \pi^- p$ and $\pi^- p \rightarrow \pi^0 n$ processes. we have defined $M_S \equiv [\frac{\omega_i}{\mu_q} + |\mathbf{A}_{in}| \frac{2|\mathbf{k}|}{3\alpha^2}] [\frac{\omega_f}{\mu_q} + |\mathbf{A}_{out}| \frac{2|\mathbf{q}|}{3\alpha^2}]$, $M_p \equiv \frac{|\mathbf{A}_{out}||\mathbf{A}_{in}|}{|\mathbf{k}||\mathbf{q}|}$, $M_{P0} \equiv [\frac{\omega_i}{\mu_q} + |\mathbf{A}_{in}| \frac{|\mathbf{k}|}{\alpha^2}] [\frac{\omega_f}{\mu_q} + |\mathbf{A}_{out}| \frac{|\mathbf{q}|}{\alpha^2}]$, $M_D \equiv |\mathbf{A}_{out}||\mathbf{A}_{in}|$, $M_{P2} \equiv [\frac{\omega_i}{\mu_q} + |\mathbf{A}_{in}| \frac{2|\mathbf{k}|}{5\alpha^2}] [\frac{\omega_f}{\mu_q} + |\mathbf{A}_{out}| \frac{2|\mathbf{q}|}{5\alpha^2}]$, $M_F \equiv |\mathbf{A}_{out}||\mathbf{A}_{in}| \frac{|\mathbf{k}||\mathbf{q}|}{9.0\alpha^4}$, $P'_j(z) \equiv \frac{\partial P_j(z)}{\partial z}$. The functions \mathbf{A}_{in} and \mathbf{A}_{out} are defined by $\mathbf{A}_{in} \equiv -(\frac{\omega_i}{E_i+M_i} + 1)\mathbf{k}$ and $\mathbf{A}_{out} \equiv -(\frac{\omega_f}{E_f+M_f} + 1)\mathbf{q}$, respectively. The μ_q is a reduced mass at the quark model level, which equals to $1/\mu_q = 2/m_u$ for πN scattering processes.

resonance	$[N_{6,}^{2S+1} N_3, n, I]$	O_R	$\pi^+ p \rightarrow \pi^+ p$	$\pi^- p \rightarrow \pi^- p$	$\pi^- p \rightarrow \pi^0 n$
$N(938)P_{11}$	$[56,^2 8, 0, 0)$	$f(\theta)$ $g(\theta)$	\dots \dots	$\frac{25}{9} \mathbf{A}_{in} \mathbf{A}_{out} P_1(z)$ $\frac{25}{9} \mathbf{A}_{in} \mathbf{A}_{out} \sin\theta P'_1(z)$	$-\frac{25\sqrt{2}}{18} \mathbf{A}_{in} \mathbf{A}_{out} P_1(z)$ $-\frac{25\sqrt{2}}{18} \mathbf{A}_{in} \mathbf{A}_{out} \sin\theta P'_1(z)$
$\Delta(1232)P_{33}$	$[56,^4 10, 0, 0)$	$f(\theta)$ $g(\theta)$	$\frac{8}{3} \mathbf{A}_{in} \mathbf{A}_{out} P_1(z)$ $-\frac{4}{3} \mathbf{A}_{in} \mathbf{A}_{out} \sin\theta P'_1(z)$	$\frac{8}{3} \mathbf{A}_{in} \mathbf{A}_{out} P_1(z)$ $-\frac{4}{3} \mathbf{A}_{in} \mathbf{A}_{out} \sin\theta P'_1(z)$	$\frac{8\sqrt{2}}{9} \mathbf{A}_{in} \mathbf{A}_{out} P_1(z)$ $-\frac{4\sqrt{2}}{9} \mathbf{A}_{in} \mathbf{A}_{out} \sin\theta P'_1(z)$
$\Delta(1620)S_{31}$	$[70,^2 10, 1, 1)$	$f(\theta)$ $g(\theta)$	$\frac{1}{24}M_S\alpha^2$ \dots	$\frac{1}{72}M_S\alpha^2$ \dots	$\frac{\sqrt{2}}{72}M_S\alpha^2$ \dots
$N(1535)S_{11}$	$[70,^2 8, 1, 1)$	$f(\theta)$ $g(\theta)$	\dots \dots	$\frac{2}{9}M_S\alpha^2$ \dots	$-\frac{4\sqrt{2}}{36}M_S\alpha^2$ \dots
$N(1650)S_{11}$	$[70,^4 8, 1, 1)$	$f(\theta)$ $g(\theta)$	\dots \dots	$\frac{1}{18}M_S\alpha^2$ \dots	$-\frac{\sqrt{2}}{36}M_S\alpha^2$ \dots
$\Delta(1700)D_{33}$	$[70,^2 10, 1, 1)$	$f(\theta)$ $g(\theta)$	$\frac{1}{27}M_D\frac{ \mathbf{k} \mathbf{q} }{\alpha^2}P_2(z)$ $\frac{1}{54}M_D\frac{ \mathbf{k} \mathbf{q} }{\alpha^2}\sin\theta P'_2(z)$	$\frac{2}{81}M_D\frac{ \mathbf{k} \mathbf{q} }{\alpha^2}P_2(z)$ $\frac{1}{81}M_D\frac{ \mathbf{k} \mathbf{q} }{\alpha^2}\sin\theta P'_2(z)$	$\frac{2\sqrt{2}}{81}M_D\frac{ \mathbf{k} \mathbf{q} }{\alpha^2}P_2(z)$ $\frac{\sqrt{2}}{81}M_D\frac{ \mathbf{k} \mathbf{q} }{\alpha^2}\sin\theta P'_2(z)$
$N(1520)D_{13}$	$[70,^2 8, 1, 1)$	$f(\theta)$ $g(\theta)$	\dots \dots	$\frac{40 \times 82}{41 \times 405}M_D\frac{ \mathbf{k} \mathbf{q} }{\alpha^2}P_2(z)$ $\frac{40 \times 82}{41 \times 810}M_D\frac{ \mathbf{k} \mathbf{q} }{\alpha^2}\sin\theta P'_2(z)$	$-\frac{40 \times 41 \sqrt{2}}{41 \times 405}M_D\frac{ \mathbf{k} \mathbf{q} }{\alpha^2}P_2(z)$ $-\frac{40 \times 41 \sqrt{2}}{41 \times 810}M_D\frac{ \mathbf{k} \mathbf{q} }{\alpha^2}\sin\theta P'_2(z)$
$N(1700)D_{13}$	$[70,^4 8, 1, 1)$	$f(\theta)$ $g(\theta)$	\dots \dots	$\frac{1 \times 82}{41 \times 405}M_D\frac{ \mathbf{k} \mathbf{q} }{\alpha^2}P_2(z)$ $\frac{1 \times 82}{41 \times 810}M_D\frac{ \mathbf{k} \mathbf{q} }{\alpha^2}\sin\theta P'_2(z)$	$-\frac{1 \times 41 \sqrt{2}}{41 \times 405}M_D\frac{ \mathbf{k} \mathbf{q} }{\alpha^2}P_2(z)$ $-\frac{1 \times 41 \sqrt{2}}{41 \times 810}M_D\frac{ \mathbf{k} \mathbf{q} }{\alpha^2}\sin\theta P'_2(z)$
$N(1675)D_{15}$	$[70,^4 8, 1, 1)$	$f(\theta)$ $g(\theta)$	\dots \dots	$\frac{2}{45}M_D\frac{ \mathbf{k} \mathbf{q} }{\alpha^2}P_2(z)$ $\frac{2}{135}M_D\frac{ \mathbf{k} \mathbf{q} }{\alpha^2}\sin\theta P'_2(z)$	$-\frac{\sqrt{2}}{45}M_D\frac{ \mathbf{k} \mathbf{q} }{\alpha^2}P_2(z)$ $-\frac{\sqrt{2}}{135}M_D\frac{ \mathbf{k} \mathbf{q} }{\alpha^2}\sin\theta P'_2(z)$
$N(1440)P_{11}$	$[56,^2 8, 2, 0)$	$f(\theta)$ $g(\theta)$	\dots \dots	$\frac{50 \times 11}{66 \times 81 \times 4}M_{P0}P_1(z)$ $\frac{50 \times 11}{66 \times 81 \times 4}M_{P0}\sin\theta P'_1(z)$	$-\frac{25 \times 11 \sqrt{2}}{33 \times 162 \times 4}M_{P0}P_1(z)$ $-\frac{25 \times 11 \sqrt{2}}{33 \times 162 \times 4}M_{P0}\sin\theta P'_1(z)$
$N(1710)P_{11}$	$[70,^2 8, 2, 0)$	$f(\theta)$ $g(\theta)$	\dots \dots	$\frac{16 \times 11}{66 \times 81 \times 4}M_{P0}P_1(z)$ $\frac{16 \times 11}{66 \times 81 \times 4}M_{P0}\sin\theta P'_1(z)$	$-\frac{8 \times 11 \sqrt{2}}{33 \times 162 \times 4}M_{P0}P_1(z)$ $-\frac{8 \times 11 \sqrt{2}}{33 \times 162 \times 4}M_{P0}\sin\theta P'_1(z)$
$\Delta(1900)P_{31}$	$[70,^2 10, 2, 0)$	$f(\theta)$ $g(\theta)$	$\frac{1}{81 \times 8}M_{P0}P_1(z)$ $\frac{1}{81 \times 8}M_{P0}\sin\theta P'_1(z)$	$\frac{1}{81 \times 24}M_{P0}P_1(z)$ $\frac{1}{81 \times 24}M_{P0}\sin\theta P'_1(z)$	$\frac{\sqrt{2}}{81 \times 24}M_{P0}P_1(z)$ $\frac{\sqrt{2}}{81 \times 24}M_{P0}\sin\theta P'_1(z)$
$\Delta(1910)P_{31}$	$[56,^4 10, 2, 2)$	$f(\theta)$ $g(\theta)$	$\frac{5}{81}M_{P2} \mathbf{k} \mathbf{q} P_1(z)$ $\frac{5}{81}M_{P2}\sin\theta \mathbf{k} \mathbf{q} P'_1(z)$	$\frac{5}{243}M_{P2} \mathbf{k} \mathbf{q} P_1(z)$ $\frac{5}{243}M_{P2}\sin\theta \mathbf{k} \mathbf{q} P'_1(z)$	$\frac{5\sqrt{2}}{243}M_{P2} \mathbf{k} \mathbf{q} P_1(z)$ $\frac{5\sqrt{2}}{243}M_{P2}\sin\theta \mathbf{k} \mathbf{q} P'_1(z)$
$N(1880)P_{11}$	$[70,^4 8, 2, 2)$	$f(\theta)$ $g(\theta)$	\dots \dots	$\frac{5}{162 \times 6}M_{P2} \mathbf{k} \mathbf{q} P_1(z)$ $\frac{5}{162 \times 6}M_{P2}\sin\theta \mathbf{k} \mathbf{q} P'_1(z)$	$-\frac{5\sqrt{2}}{162 \times 12}M_{P2} \mathbf{k} \mathbf{q} P_1(z)$ $-\frac{5\sqrt{2}}{162 \times 12}M_{P2}\sin\theta \mathbf{k} \mathbf{q} P'_1(z)$
$\Delta(1600)P_{33}$	$[56,^4 10, 2, 0)$	$f(\theta)$ $g(\theta)$	$\frac{2}{81}M_{P0} \mathbf{k} \mathbf{q} P_1(z)$ $-\frac{1}{81}M_{P0}\sin\theta \mathbf{k} \mathbf{q} P'_1(z)$	$\frac{2}{243}M_{P0} \mathbf{k} \mathbf{q} P_1(z)$ $-\frac{1}{243}M_{P0}\sin\theta \mathbf{k} \mathbf{q} P'_1(z)$	$\frac{2\sqrt{2}}{243}M_{P0} \mathbf{k} \mathbf{q} P_1(z)$ $-\frac{\sqrt{2}}{243}M_{P0}\sin\theta \mathbf{k} \mathbf{q} P'_1(z)$
$N(?)P_{13}$	$[70,^4 8, 2, 0)$	$f(\theta)$ $g(\theta)$	\dots \dots	$\frac{1}{162 \times 3}M_{P0} \mathbf{k} \mathbf{q} P_1(z)$ $-\frac{1}{162 \times 6}M_{P0}\sin\theta \mathbf{k} \mathbf{q} P'_1(z)$	$-\frac{\sqrt{2}}{162 \times 6}M_{P0} \mathbf{k} \mathbf{q} P_1(z)$ $\frac{\sqrt{2}}{162 \times 12}M_{P0}\sin\theta \mathbf{k} \mathbf{q} P'_1(z)$
$N(1720)P_{13}$	$[56,^2 8, 2, 2)$	$f(\theta)$ $g(\theta)$	\dots \dots	$\frac{25 \times 17}{34 \times 162 \times 3}M_{P2} \mathbf{k} \mathbf{q} P_1(z)$ $-\frac{25 \times 17}{34 \times 162 \times 6}M_{P2}\sin\theta \mathbf{k} \mathbf{q} P'_1(z)$	$-\frac{25 \times 5 \times 17 \sqrt{2}}{34 \times 162 \times 12}M_{P2} \mathbf{k} \mathbf{q} P_1(z)$ $\frac{25 \times 5 \times 17 \sqrt{2}}{34 \times 162 \times 12}M_{P2}\sin\theta \mathbf{k} \mathbf{q} P'_1(z)$

nucleon parameters and phase shifts by dispersion relations, Rev. Mod. Phys. **35**, 737 (1963).

- [63] M. L. Goldberger and S. B. Treiman, Decay of the π meson, Phys. Rev. **110**, 1178 (1958).
- [64] M. M. Pavan *et al.*, Precision pion-proton elastic differential cross-sections at energies spanning the Delta resonance, Phys. Rev. C **64**, 064611 (2001).
- [65] P. J. Bussey, J. R. Carter, D. R. Dance, D. V. Bugg, A. A. Carter and A. M. Smith, πp elastic scattering from 88 to 292 MeV, Nucl. Phys. B **58**, 363 (1973).
- [66] V. A. Gordeev *et al.*, Measurement of differential cross-sections of $\pi^+ P$ and $\pi^- P$ elastic scattering in the region of low lying pion nucleon resonances, Nucl. Phys. A **364**, 408 (1981).
- [67] M. E. Sadler, W. J. Briscoe, D. H. Fitzgerald, B. M. K. Nefkens and C. J. Sefor, Differential cross-sections for $\pi^+ P$ and $\pi^- P$ elastic scattering from 378 MeV/c to 687 MeV/c, Phys. Rev. D **35**, 2718 (1987).
- [68] R. C. Minehart, J. S. Boswell, J. F. Davis, D. Day, J. S. McCarthy, R. R. Whitney, H. J. Ziock and E. A. Wadlinger, Pion deuteron elastic scattering for momenta from 408 MeV/c to 600 MeV/c, Phys. Rev. Lett. **46**, 1185 (1981).
- [69] J. C. Comiso, D. J. Blasberg, R. P. Haddock, B. M. K. Nefkens, P. Truol and L. J. Verhey, Differential cross-section measurements of $\pi^- p \rightarrow \pi^0 n$ around the $P_{33}(1232)$ resonance, Phys. Rev. D **12**, 738 (1975).
- [70] P. A. Berardo, R. P. Haddock, B. M. K. Nefkens, L. J. Verhey,

TABLE V: A continuation of Table IV.

Resonance	$[N_6, {}^{2S+1}N_3, n, I]$	O_R	$\pi^+ p \rightarrow \pi^+ p$	$\pi^- p \rightarrow \pi^- p$	$\pi^- p \rightarrow \pi^0 n$
$\Delta(1920)P_{33}$	$[56, {}^4 10, 2, 2)$	$f(\theta)$ $g(\theta)$	$\frac{5}{81} M_{P2} \mathbf{k} \mathbf{q} P_1(z)$ $-\frac{5}{162} M_{P2} \sin \theta \mathbf{k} \mathbf{q} P'_1(z)$	$\frac{5}{81 \times 3} M_{P2} \mathbf{k} \mathbf{q} P_1(z)$ $-\frac{5}{162 \times 3} M_{P2} \sin \theta \mathbf{k} \mathbf{q} P'_1(z)$	$\frac{5\sqrt{2}}{81 \times 3} M_{P2} \mathbf{k} \mathbf{q} P_1(z)$ $-\frac{5\sqrt{2}}{162 \times 3} M_{P2} \sin \theta \mathbf{k} \mathbf{q} P'_1(z)$
$N(1900)P_{13}$	$[70, {}^2 8, 2, 2)$	$f(\theta)$ $g(\theta)$	\dots \dots	$\frac{8 \times 17}{34 \times 162 \times 3} M_{P2} \mathbf{k} \mathbf{q} P_1(z)$ $-\frac{8 \times 17}{34 \times 162 \times 6} M_{P2} \sin \theta \mathbf{k} \mathbf{q} P'_1(z)$	$-\frac{16 \times 5 \times 17 \sqrt{2}}{34 \times 162 \times 12} M_{P2} \mathbf{k} \mathbf{q} P_1(z)$ $\frac{8 \times 5 \times 17 \sqrt{2}}{34 \times 162 \times 12} M_{P2} \sin \theta \mathbf{k} \mathbf{q} P'_1(z)$
$N(?)P_{13}$	$[70, {}^4 8, 2, 2)$	$f(\theta)$ $g(\theta)$	\dots \dots	$\frac{1 \times 17}{34 \times 162 \times 3} M_{P2} \mathbf{k} \mathbf{q} P_1(z)$ $-\frac{1 \times 17}{34 \times 162 \times 6} M_{P2} \sin \theta \mathbf{k} \mathbf{q} P'_1(z)$	$-\frac{2 \times 5 \times 17 \sqrt{2}}{34 \times 162 \times 12} M_{P2} \mathbf{k} \mathbf{q} P_1(z)$ $\frac{1 \times 5 \times 17 \sqrt{2}}{34 \times 162 \times 12} M_{P2} \sin \theta \mathbf{k} \mathbf{q} P'_1(z)$
$\Delta(?)P_{33}$	$[70, {}^2 10, 2, 2)$	$f(\theta)$ $g(\theta)$	$\frac{5}{81 \times 8} M_{P2} \mathbf{k} \mathbf{q} P_1(z)$ $-\frac{5}{162 \times 8} M_{P2} \sin \theta \mathbf{k} \mathbf{q} P'_1(z)$	$\frac{5}{81 \times 24} M_{P2} \mathbf{k} \mathbf{q} P_1(z)$ $-\frac{5}{162 \times 24} M_{P2} \sin \theta \mathbf{k} \mathbf{q} P'_1(z)$	$\frac{5\sqrt{2}}{81 \times 24} M_{P2} \mathbf{k} \mathbf{q} P_1(z)$ $-\frac{5\sqrt{2}}{162 \times 24} M_{P2} \sin \theta \mathbf{k} \mathbf{q} P'_1(z)$
$N(1680)F_{15}$	$[56, {}^2 8, 2, 2)$	$f(\theta)$ $g(\theta)$	\dots \dots	$\frac{175 \times 233}{233 \times 18 \times 35} M_F \mathbf{k} \mathbf{q} P_3(z)$ $-\frac{175 \times 233}{233 \times 54 \times 35} M_F \sin \theta \mathbf{k} \mathbf{q} P'_3(z)$	$-\frac{175 \times 233 \sqrt{2}}{233 \times 36 \times 35} M_F \mathbf{k} \mathbf{q} P_3(z)$ $-\frac{175 \times 233 \sqrt{2}}{233 \times 108 \times 35} M_F \sin \theta \mathbf{k} \mathbf{q} P'_3(z)$
$\Delta(1880)F_{35}$	$[56, {}^4 10, 2, 2)$	$f(\theta)$ $g(\theta)$	$\frac{16 \times 23}{23 \times 12 \times 35} M_F \mathbf{k} \mathbf{q} P_3(z)$ $\frac{16 \times 23}{23 \times 36 \times 35} M_F \sin \theta \mathbf{k} \mathbf{q} P'_3(z)$	$\frac{16 \times 23}{23 \times 36 \times 35} M_F \mathbf{k} \mathbf{q} P_3(z)$ $\frac{16 \times 23}{23 \times 108 \times 35} M_F \sin \theta \mathbf{k} \mathbf{q} P'_3(z)$	$\frac{16 \times 23 \sqrt{2}}{23 \times 36 \times 35} M_F \mathbf{k} \mathbf{q} P_3(z)$ $\frac{16 \times 23 \sqrt{2}}{23 \times 108 \times 35} M_F \sin \theta \mathbf{k} \mathbf{q} P'_3(z)$
$N(1860)F_{15}$	$[70, {}^2 8, 2, 2)$	$f(\theta)$ $g(\theta)$	\dots \dots	$\frac{56 \times 233}{233 \times 18 \times 35} M_F \mathbf{k} \mathbf{q} P_3(z)$ $-\frac{56 \times 233}{233 \times 54 \times 35} M_F \sin \theta \mathbf{k} \mathbf{q} P'_3(z)$	$-\frac{56 \times 233 \sqrt{2}}{233 \times 36 \times 35} M_F \mathbf{k} \mathbf{q} P_3(z)$ $-\frac{56 \times 233 \sqrt{2}}{233 \times 108 \times 35} M_F \sin \theta \mathbf{k} \mathbf{q} P'_3(z)$
$N(?)F_{15}$	$[70, {}^4 8, 2, 2)$	$f(\theta)$ $g(\theta)$	\dots \dots	$\frac{2 \times 233}{233 \times 18 \times 35} M_F \mathbf{k} \mathbf{q} P_3(z)$ $\frac{2 \times 233}{233 \times 54 \times 35} M_F \sin \theta \mathbf{k} \mathbf{q} P'_3(z)$	$-\frac{2 \times 233 \sqrt{2}}{233 \times 36 \times 35} M_F \mathbf{k} \mathbf{q} P_3(z)$ $-\frac{2 \times 233 \sqrt{2}}{233 \times 108 \times 35} M_F \sin \theta \mathbf{k} \mathbf{q} P'_3(z)$
$\Delta(2000)F_{35}$	$[70, {}^2 10, 2, 2)$	$f(\theta)$ $g(\theta)$	$\frac{7 \times 23}{23 \times 12 \times 35} M_F \mathbf{k} \mathbf{q} P_3(z)$ $\frac{7 \times 23}{23 \times 36 \times 35} M_F \sin \theta \mathbf{k} \mathbf{q} P'_3(z)$	$\frac{7 \times 23}{23 \times 36 \times 35} M_F \mathbf{k} \mathbf{q} P_3(z)$ $\frac{7 \times 23}{23 \times 108 \times 35} M_F \sin \theta \mathbf{k} \mathbf{q} P'_3(z)$	$\frac{7 \times 23 \sqrt{2}}{23 \times 36 \times 35} M_F \mathbf{k} \mathbf{q} P_3(z)$ $\frac{7 \times 23 \sqrt{2}}{23 \times 108 \times 35} M_F \sin \theta \mathbf{k} \mathbf{q} P'_3(z)$
$\Delta(?)F_{37}$	$[56, {}^2 10, 2, 2)$	$f(\theta)$ $g(\theta)$	$\frac{8}{35} M_F \mathbf{k} \mathbf{q} P_3(z)$ $-\frac{2}{35} M_F \sin \theta \mathbf{k} \mathbf{q} P'_3(z)$	$\frac{8}{105} M_F \mathbf{k} \mathbf{q} P_3(z)$ $-\frac{2}{105} M_F \sin \theta \mathbf{k} \mathbf{q} P'_3(z)$	$\frac{8\sqrt{2}}{105} M_F \mathbf{k} \mathbf{q} P_3(z)$ $-\frac{2\sqrt{2}}{105} M_F \sin \theta \mathbf{k} \mathbf{q} P'_3(z)$
$N(?)F_{17}$	$[70, {}^4 8, 2, 2)$	$f(\theta)$ $g(\theta)$	\dots \dots	$\frac{2}{105} M_F \mathbf{k} \mathbf{q} P_3(z)$ $-\frac{1}{210} M_F \sin \theta \mathbf{k} \mathbf{q} P'_3(z)$	$-\frac{\sqrt{2}}{210} M_F \mathbf{k} \mathbf{q} P_3(z)$ $\frac{\sqrt{2}}{420} M_F \sin \theta \mathbf{k} \mathbf{q} P'_3(z)$

M. E. Zeller, A. S. L. Parsons and P. Truoe, Measurement of the differential cross-section for $\pi^- p \rightarrow \pi^0 n$ at 317, 452, and 491 MeV/c, Phys. Rev. D **6**, 756 (1972).

- [71] M. E. Sadler *et al.* [Crystal Ball Collaboration], Differential cross-section of the charge exchange reaction $\pi^- p \rightarrow \pi^0 n$ in the momentum range from 148 MeV/c to 323 MeV/c, Phys. Rev. C **69**, 055206 (2004).
- [72] R. F. Jenefsky *et al.*, Measurement of the differential cross-section for $\pi^- p \rightarrow \pi^0 n$ around the $\Delta(1232)$ resonance and test of the charge independence principle, Nucl. Phys. A **290**, 407 (1977).
- [73] M. G. Hauser, K. W. Chen and P. A. Crean, New evidence for the $P_{11}(1470)$ resonance in $\pi^- p \rightarrow \pi^0 n$ below 600 MeV, Phys. Lett. B **35**, 252 (1971).
- [74] C. V. Gaulard *et al.*, Analyzing powers for the $\pi^- p \rightarrow \pi^0 n$ reaction across the $\Delta(1232)$ resonance, Phys. Rev. C **60**, 024604 (1999).
- [75] G. J. Hofman *et al.*, Analyzing powers for $\pi^\pm p$ polarized elastic scattering between 87 MeV and 263 MeV, Phys. Rev. C **58**, 3484 (1998).
- [76] M. E. Sevier *et al.*, Analyzing powers in $\pi^\pm P$ (polarized) elastic scattering from $T_\pi=98$ MeV to 263 MeV, Phys. Rev. C **40**, 2780 (1989).
- [77] A. Bosshard *et al.*, Analyzing power in pion proton bremsstrahlung, and the $\Delta^{++}(1232)$ magnetic moment, Phys. Rev. D **44**, 1962 (1991).
- [78] I. Supek *et al.*, Spin rotation parameters A and R for $\pi^+ p$ and $\pi^- p$ elastic scattering from 427 MeV/c to 657 MeV/c, Phys. Rev. D **47**, 1762 (1993).
- [79] A. Mokhtari, A. D. Eichon, G. J. Kim, B. M. K. Nefkens, J. A. Wightman, D. H. Fitzgerald, W. J. Briscoe and M. E. Sadler, Analyzing power and transversity cross-sections for $\pi^+ P$ and $\pi^- P$ elastic scattering from 471 MeV/c to 687 MeV/c, Phys. Rev. D **35**, 810 (1987).
- [80] L. Dubal *et al.*, Measurement of the polarization parameter in $\pi^+ p$ scattering at 291.4 MeV and 310 MeV, Helv. Phys. Acta **50**, 815 (1977).
- [81] V. V. Abaev *et al.*, Measurement of the polarization parameter P in $\pi^+ p$ elastic scattering in the region Of low lying pion-nucleon resonances, Z. Phys. A **311**, 217 (1983).
- [82] C. Amsler, F. Rudolf, P. Weymuth, L. Dubal, G. H. Eaton, R. Frosch, S. Mango and F. Pozar, Measurement and phase shift analysis of the P parameter in $\pi^+ p$ scattering at 236 MeV, Phys. Lett. B **57**, 289 (1975).
- [83] C. B. Chiu *et al.*, Pion-Proton Charge-Exchange Scattering from 500 to 1300 MeV, Phys. Rev. **156**, 1415 (1967).
- [84] F. Bulos *et al.*, Charge exchange and production of eta mesons and multiple neutral pions in pi-p reactions between 654 and 1247 mev/c, Phys. Rev. **187**, 1827 (1969).
- [85] J. Breitschopf *et al.*, Pionic charge exchange on the proton from 40 MeV to 250 MeV, Phys. Lett. B **639**, 424 (2006).
- [86] L. Y. Xiao and X. H. Zhong, Ξ baryon strong decays in a chiral quark model, Phys. Rev. D **87**, 094002 (2013).
- [87] T. Sato and T. S. H. Lee, Dynamical study of the Delta excitation in $N(e, e' \pi)$ reactions, Phys. Rev. C **63**, 055201 (2001).
- [88] K. Bermuth, D. Drechsel, L. Tiator and J. B. Seaborn, Photoproduction of Δ and Roper resonances in the cloudy bag model, Phys. Rev. D **37**, 89 (1988).
- [89] D. H. Lu, A. W. Thomas and A. G. Williams, A chiral bag model approach to delta electroproduction, Phys. Rev. C **55**, 3108 (1997).
- [90] A. Faessler, T. Gutsche, B. R. Holstein, V. E. Lyubovitskij, D. Nicmorus and K. Pumsa-ard, Light baryon magnetic moments and $N \rightarrow \Delta \gamma$ transition in a Lorentz covariant chiral

- quark approach, Phys. Rev. D **74**, 074010 (2006).
- [91] I. G. Aznauryan and V. D. Burkert, Electroexcitation of the $\Delta(1232)_{\frac{3}{2}}^{+}$ and $\Delta(1600)_{\frac{3}{2}}^{+}$ in a light-front relativistic quark model, Phys. Rev. C **92**, 035211 (2015).
- [92] T. Sekihara, T. Arai, J. Yamagata-Sekihara and S. Yasui, Compositeness of baryonic resonances: Application to the $\Delta(1232)$, $N(1535)$, and $N(1650)$ resonances, Phys. Rev. C **93**, 035204 (2016).
- [93] J.F.Arens *et al.*, Measurement of polarization in $\pi^{-}p$ elastic scattering from 229 to 390 MeV, Phys. Rev. **167**, 1261 (1968).
- [94] J. C. Alder *et al.*, Measurement of the asymmetry parameter A in $\pi^{-}p$ elastic and charge exchange scattering at pion energies $T_{\pi}=98$ MeV, 238 MeV, 292 MeV, and 310 MeV, Phys. Rev. D **27**, 1040 (1983).
- [95] G. J. Hofman *et al.*, Analyzing powers for $\pi^{-}p$ elastic scattering at 279 MeV, Phys. Rev. C **68**, 018202 (2003).
- [96] J. J. Goergen *et al.*, Analyzing powers for the reaction $\pi^{-}p \rightarrow \pi^{0}n$ at $T_{\pi}=161$ MeV, Phys. Rev. D **42**, 2374 (1990).
- [97] G. J. Kim, J. Arends, J. Engelage, B. M. K. Nefkens, H. J. Ziock, W. J. Briscoe, M. Taragin and M. E. Sadler, Analyzing power for $\pi^{-}p$ charge exchange in the backward hemisphere from 301 MeV/c to 625 MeV/c and a test of πN partial wave analyses, Phys. Rev. D **41**, 733 (1990).
- [98] R. E. Hill, N. E. Booth, R. J. Esterling, D. A. Jenkins, N. H. Lipman, H. R. Ruge and O. T. Vik, Neutron polarization in $\pi^{-}p$ charge-exchange scattering at 310 MeV, Phys. Rev. D **2**, 1199 (1970).
- [99] J. B. Cheze, N. Codreanu, J. L. Hamel, O. Le Calvez, J. Teiger, B. Thevenet, H. Zaccane and J. Zsembery, Measurement of the $\pi^{-}p \rightarrow \pi^{0}n$ and $\pi^{-}p \rightarrow n\gamma$ differential cross-sections near the resonance $P_{11}(1460)$, Nucl. Phys. B **72**, 365 (1974).
- [100] D. E. Bayadilov *et al.*, Measurement of differential cross sections for charge-exchange $\pi^{-}p$ scattering in the region of small scattering angles, Phys. Atom. Nucl. **67**, 493 (2004) [Yad. Fiz. **67**, 512 (2004)].
- [101] I. V. Lopatin, Measurement of the differential cross-sections for $\pi^{-}p$ charge-exchange scattering in the region of the low lying P_{11} , S_{11} , and D_{13} resonances, Phys. Atom. Nucl. **65**, 236 (2002) [Yad. Fiz. **65**, 260 (2002)].
- [102] B. Julia-Diaz, D. O. Riska and F. Coester, Axial transition form-factors and pion decay of baryon resonances, Phys. Rev. C **70**, 045204 (2004).
- [103] T. Melde, W. Plessas and R. F. Wagenbrunn, Covariant calculation of mesonic baryon decays, Phys. Rev. C **72**, 015207 (2005) Erratum: [Phys. Rev. C **74**, 069901 (2006)].
- [104] B. S. Zou and D. O. Riska, The $s\bar{s}$ component of the proton and the strangeness magnetic moment, Phys. Rev. Lett. **95**, 072001 (2005).
- [105] B. S. Zou, Five-quark components in baryons, Nucl. Phys. A **835**, 199 (2010).
- [106] Q. B. Li and D. O. Riska, The role of $q\bar{q}$ components in the $N(1440)$ resonance, Phys. Rev. C **74**, 015202 (2006).
- [107] B. Julia-Diaz and D. O. Riska, The role of $qqq\bar{q}$ components in the nucleon and the $N(1440)$ resonance, Nucl. Phys. A **780**, 175 (2006).
- [108] J. Gegelia, U. G. Meißner and D. L. Yao, The width of the Roper resonance in baryon chiral perturbation theory, Phys. Lett. B **760**, 736 (2016).
- [109] I. T. Obukhovskiy, A. Faessler, T. Gutsche and V. E. Lyubovitskij, Electromagnetic structure of the nucleon and the Roper resonance in a light-front quark approach, Phys. Rev. D **89**, 014032 (2014).
- [110] I. T. Obukhovskiy, A. Faessler, D. K. Fedorov, T. Gutsche and V. E. Lyubovitskij, Electroproduction of the Roper resonance on the proton: the role of the three-quark core and the molecular $N\sigma$ component, Phys. Rev. D **84**, 014004 (2011).
- [111] S. G. Yuan, C. S. An and J. He, Contributions of $qqq\bar{q}$ components to axial charges of proton and $N(1440)$, Commun. Theor. Phys. **54**, 697 (2010).
- [112] L. S. Kisslinger and Z. P. Li, Hybrid baryons via QCD sum rules, Phys. Rev. D **51**, R5986 (1995).
- [113] Z. W. Liu, W. Kamleh, D. B. Leinweber, F. M. Stokes, A. W. Thomas and J. J. Wu, Hamiltonian effective field theory study of the $N^{*}(1440)$ resonance in lattice QCD, arXiv:1607.04536 [nucl-th].
- [114] C. B. Lang, L. Leskovec, M. Padmanath and S. Prelovsek, Pion-nucleon scattering in the Roper channel from lattice QCD, Phys. Rev. D **95**, 014510 (2017).